Multi-Target CFTR Modulators Endowed with Multiple Beneficial Side Effects for Cystic Fibrosis Patients: Toward a Simplified Therapeutic Approach

Sabrina Tassini,[a] Emily Langron,[c] Leen Delang,[b] Carmen Mirabelli,[b] Kristina Lanko,[b] Emmanuele Crespan,[d] Miroslava Kissova,[d] Giulia Tagliavini,[d] Greta Fontò,[a] Simona Bertoni,[a] Simone Palese,[a] Carmine Giorgio,[a] Francesca Ravanetti,[e] Luisa Ragionieri,[e] Giovanni Maga,[d] Paola Vergani,[c] Johan Neyts,[b] and Marco Radi[a,*]

[Ω]This *article is dedicated to the memory of prof. Maurizio Botta, a mentor and friend who inspired everyone who knew him with his unique vision for research and innovation; his legacy will live on.*

[a] Dipartimento di Scienze degli Alimenti e del Farmaco, Università degli Studi di Parma, Viale delle Scienze, 27/A, 43124 Parma, Italy

[b] Laboratory of Virology and Experimental Chemotherapy, Rega Institute for Medical Research, KU Leuven, Minderbroedersstraat 10, 3000, Leuven, Belgium

[c] Department of Neuroscience, Physiology and Pharmacology, University College London, Gower Street, WC1E 6BT London, UK

[d] Istituto di Genetica Molecolare, IGM-CNR, Via Abbiategrasso 207, 27100 Pavia, Italy

[e] Dipartimento di Scienze Medico-Veterinarie, Università degli Studi di Parma, Via del Taglio 10, 43126 Parma, Italy

KEYWORDS: F508del-CFTR, cystic fibrosis, multi-target, PI4KIIIβ, broad-spectrum antivirals, enterovirus.

ABSTRACT

Cystic fibrosis (CF) is a multi-organ protein misfolding disease caused by mutations of the cystic fibrosis transmembrane conductance regulator (CFTR). In addition to respiratory impairment due to mucus accumulation, viruses, bacteria and their co-infections are recognized triggers of acute pulmonary exacerbations, accelerating disease progression, and increasing hospitalization and mortality rate. Treatment complexity increases with the age of patients, as do the number and severity of side effects, drug-drug interactions and costs. Simplifying the therapeutic regimen represents therefore one of the key priorities of CF treatment. We have recently reported the discovery of multitarget compounds able to "kill two birds with one stone" by targeting F508del-CFTR and PI4KIIIβ and thus acting simultaneously as mild correctors and broad-spectrum picornavirus inhibitors. Starting from the previously identified multitarget hits, we report herein the synthesis and biological profiling of new bithiazole derivatives to elucidate the structural requirements to improve F508del-CFTR correction and antiviral potencies. The most promising compound **23a** inhibited PI4KIIIβ and selected picornaviruses (EV71, CVB3, hRV02), showed good F508del-CFTR correction potency, additivity and possible synergy with lumacaftor (VX809) at low micromolar concentration. In addition, it was well tolerated *in vivo* by C57BL/6 mice with no sign of acute toxicity and histological alterations in key biodistribution organs.

INTRODUCTION

Cystic fibrosis (CF) is a common lethal autosomal recessive disease caused by mutations affecting the cystic fibrosis transmembrane conductance regulator (CFTR), a cAMP-regulated anion-selective channel expressed in various epithelia such as those of airways, intestinal tract, pancreas ducts, testes and sweat glands. About 90% of cystic fibrosis patients are either heterozygous or homozygous for a CFTR protein lacking phenylalanine 508 (ΔF508-CFTR).[1] The ΔF508 mutant is largely unable to exit the endoplasmic reticulum.[2,3] Only a small fraction of the synthesized protein reaches the plasma membrane (trafficking defect). However, when targeted to the plasma membrane, the ΔF508 protein also shows an accelerated rate of internalization and an intrinsic low channel activity compared to wild type CFTR.[4] Low anion flow due to mutated CFTR, causes reduced fluid secretion and accumulation of abnormally thick mucus that clogs the ducts and favors the development of bacterial/viral infections. CF epithelial cell vulnerability and dysregulation of the local inflammatory responses lead to more severe viral infections and appear to render the airway even more prone to bacterial infection, leading to pulmonary exacerbations that accelerate disease progression, impair quality of life, increase hospitalization and mortality rate.[5-7] To reduce symptoms and slow organ deterioration, patients receive multiple treatments (antibiotics, steroids, mucolytics, bronchodilators, pancreatic enzymes) and undergo a daily physical exercise regimen including physiotherapy to loosen and remove airway mucus. This complex regimen, combined with patients' comorbidities, makes therapeutic burden and drug-drug interactions important issues in CF care.[8-11] Over the years, there has been an intensive effort to find drugs acting on the root cause of the disease: lumacaftor (VX-809) and tezacaftor (VX-661) are pharmacological chaperones that correct the folding defect and improve trafficking of the , while ivacaftor (VX-770) is a small molecule acting as a potentiator of the channel's conductance.[12-14] However,

F508del-CFTR patients do not benefit from monotherapy with these agents, providing only ~4% improvement in lung function measured as improvement in FEV1 percentage predicted. On the other hand, the combination of a corrector (lumacaftor) with a potentiator (ivacaftor), marketed as Orkambi™, has provided minimal health benefits for people ages 12 and older, which were homozygous for the F508del-CFTR mutation.[15] In addition to the poor effectiveness of Orkambi™ in F508del-CFTR bearing patients, lumacaftor negatively interacted with ivacaftor, increasing its metabolism and thus requiring a higher dose of the latter when used in combination as Orkambi, while Ivacaftor reduces F508del-CFTR surface expression.[16-18] Recently, the positive effect of combination treatments in correcting F508del-CFTR has been highlighted by Carlile et al. by showing that a triple combination of correctors (MCG1516A, RDR1 and VX-809) binding to different pockets on CFTR, yielded a functional expression of the channel that was approximately 90% of wild-type's.[19] Even if drug combinations seem to be the right approach for optimal F508del-CFTR functional expression, drug-drug interactions (e.g. lumacaftor-ivacaftor, macrolides-lumacaftor/ivacaftor) represent a serious risk and must be taken into account for a safe and efficient CF therapy.[16]

Considering the poor efficacy of current therapeutic treatments for F508del-CFTR, the CF therapeutic burden, the severity of viral infections in CF and their role in facilitating bacterial colonization,[20,21] our research group has recently approached this complex disease by developing multitarget compounds able to simultaneously act as correctors of the F508del-CFTR folding defect and as broad-spectrum antivirals.[22] Here we report the synthesis and biological profiling of new bithiazole derivatives to elucidate the structural requirements needed to improve both F508del-CFTR correction and antiviral potencies. Among the synthesized compounds, **23a-c** showed a dual effect on F508del-CFTR, increasing the membrane expression (in a pHTomato assay) and channel function. They had a corrector effect additive to VX-809's, increasing the F508del-CFTR membrane density three-fold more

thanVX-809 alone. The most promising compound **23a** was well tolerated in acute toxicity studies conducted on C57BL/6 mice, with no sign of histological alterations in gut, lung and liver parenchyma.

RESULTS AND DISCUSSION

Over the past decade, the "one-drug, one-gene, one-disease" paradigm has been questioned, based also on functional genomic studies showing that single-gene knockouts gave a phenotypic response in a low percentage of cases, due to redundancy and compensatory signaling of biological networks.[23-25] It has been proposed that partial inhibition of multiple biological targets with a single (multi-target) drug, the so called polypharmacology approach, is more effective than full inhibition of a single target, reducing target-related toxicity and attrition rate in clinical development.[26] This "one-drug, multiple-targets" approach is quite valuable in the treatment of a complex disease like cystic fibrosis, which is characterized by a high drug-burden, virus/bacteria-related exacerbations and poor efficacy of current treatments, especially for patients bearing the F508del-CFTR mutation. Recently, we used a combined virtual docking/similarity clustering approach to identify, for the first time, single compounds acting as broad-spectrum antivirals and correctors of the F508del-CFTR folding defect.[22] We reasoned that the best way to kill two birds with one stone is if the birds are closed in the same cage: out of the metaphor, we focused on two targets (PI4KIIIβ and F508del-CFTR) that are localized within the endoplasmic reticulum (ER) to avoid additional problems of delivering the compound to different locations/compartments. On one side, our multi-target molecule will enter the ER and bind F508del-CFTR (like structurally related Corr-4a does)[27] to correct the folding defect. On the other hand, once inside the ER this molecule will also inhibit PI4KIIIβ to interfere with the replication of Picornaviruses and may also facilitate restoration of airway surface liquid (ASL) fluidity by indirectly downmodulating epithelial Na(+) channel (ENaC)

activity via reduction of $PI(4,5)P_2$ concentration.[28] In addition, PI4KIIIβ inhibition by the same multi-target compound may work as alternative immunosuppressive approach to overcome acute cellular rejection (ACR) in CF patients who have received lung transplant.[29] Here we started by analyzing the structure-activity relationship (SAR) of previously published multi-target compounds against PI4KIIIβ: as shown in the upper part of Figure 1, the central bithiazole scaffold was fundamental for biological activity, while small aliphatic amide moieties (MeCONH, EtCONH, *t*BuCONH) on the left part improved activity and selectivity. Different substituents on the right part of the molecule did not much change the activity against PI4KIIIβ, although only a few modifications were attempted. Subsequently, we focused our multidimensional SAR analysis on the most promising multi-target compounds previously developed by us (**1-4**) in comparison with the known corrector **5** (Corr-4a) (Figure 1, lower part) which was not further developed because of the high toxic effect and low *in vivo* efficacy.[30] The latter compound was synthesized as described in literature[31] and submitted to the same panel of biological assays used for compounds **1-4**.[22] As described in Figure 1, we analyzed the *in vitro* activities of the selected compounds *i)* against a panel of picornaviruses representative of all major groups; ii) against lipid kinases PI4KIIIβ/ PI4KIIIα/ PI3Kα and iii) as F508del-CFTR correctors. Key efficiency metrics were also computed using Datawarrior[32]: lipophilic ligand efficiency (LLE), lipophilicity-corrected ligand efficiency (LELP) and cLogP (Figure 2). As reported by Tarcsay et al., marketed drugs and advanced clinical candidates are characterized by LELP<10 and LLE>5.[33] It emerged that small changes in the functionalization of the bithiazole scaffold may be sufficient to convert the pure corrector **5** into the multi-target compounds **1-4**, whose F508del-CFTR correction potency increased with the bulkiness of the left amide moiety. However, too bulky amide moieties (e.g. substituted aromatics) decreased the PI4KIIIβ inhibition and consequently abolished the activity against Picornaviruses. The best compromise between lipid kinase inhibition/selectivity and F508del-CFTR correction

efficacy was obtained with the *tert*-butyl amide moiety as in compound **2**. Looking at the calculated metrics, Corr-4a was predicted to be very lipophilic and this may account for its toxic effect. Among compounds **1-4**, LLE and LELP parameters indicated compounds **1** and **2** as the most promising starting point for optimization. Considering the incomplete SAR previously obtained by modifying compound **1** on the right part of the bithiazole scaffold and aiming for less lipophilic compounds, we decided to replace the right aromatic ring with different aliphatic moieties.

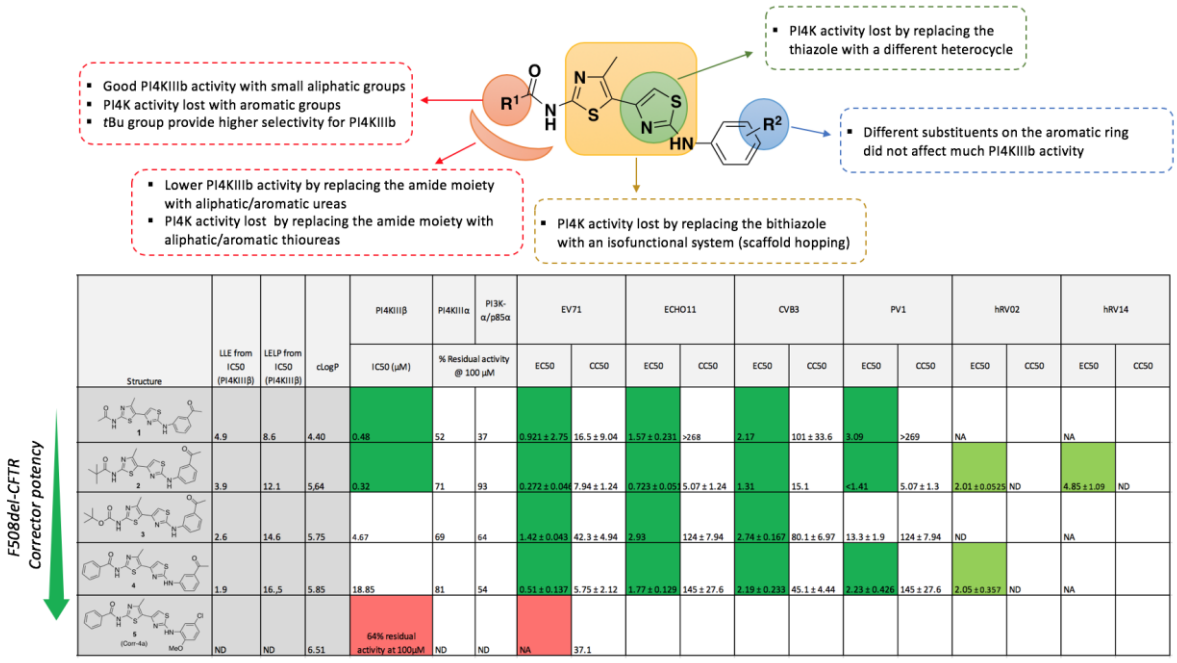

Structure	LLE from IC50 (PI4KIIIβ)	LELP from IC50 (PI4KIIIβ)	cLogP	PI4KIIIβ IC50 (μM)	PI4KIIIα % Residual activity @ 100 μM	PI3K-α/p85α % Residual activity @ 100 μM	EV71 EC50	EV71 CC50	ECHO11 EC50	ECHO11 CC50	CVB3 EC50	CVB3 CC50	PV1 EC50	PV1 CC50	hRV02 EC50	hRV02 CC50	hRV14 EC50	hRV14 CC50
1	4.9	8.6	4.40	0.48	52	37	0.921 ± 2.75	16.5 ± 9.04	1.57 ± 0.231	>268	2.17	101 ± 33.6	3.09	>269	NA		NA	
2	3.9	12.1	5,64	0.32	71	93	0.272 ± 0.04	7.94 ± 1.24	0.723 ± 0.05	5.07 ± 1.24	1.31	15.1	<1.41	5.07 ± 1.3	2.01 ± 0.0525	ND	4.85 ± 1.09	ND
3	2.6	14.6	5.75	4.67	69	64	1.42 ± 0.043	42.3 ± 4.94	2.93	124 ± 7.94	2.74 ± 0.167	80.1 ± 6.97	13.3 ± 1.9	124 ± 7.94	ND		NA	
4	1.9	16,5	5.85	18.85	81	54	0.51 ± 0.137	5.75 ± 2.12	1.77 ± 0.129	145 ± 27.6	2.19 ± 0.233	45.1 ± 4.44	2.23 ± 0.426	145 ± 27.6	2.05 ± 0.357	ND	NA	
5 (Corr-4a)	ND	ND	6.51	64% residual activity at 100μM	ND	ND	NA	37.1										

Figure 1. Multidimensional SAR of selected multi-target bithiazoles **1-4** compared to CFTR corrector **5** (Corr-4a). Biological activity was evaluated against lipid kinases (PI4KIIIβ/ PI4KIIIα/PI3Kα), F508del-CFTR correction and selected picornaviruses: enterovirus 71 (EV71), coxsackievirus B3, poliovirus 1 (PV1), human rhinovirus 2 (hRV02), human rhinovirus 14 (hRV14). EC_{50} and CC_{50} values expressed in μM.

To obtain the desired compounds **9a-d**, the bromo-derivative **8**, previously prepared,[22] was refluxed with the substituted thioureas **7a-d** as described in Scheme 1. The synthesis of **7a-d**

from the corresponding primary and secondary amines **6a-d** is outlined in the Supporting Info. We also evaluated the possibility of irreversibly inhibiting PI4KIIIβ, considering that wortmannin is a potent inhibitor of PI3K isoforms, binding covalently to the ε-amino group of LYS802 in the catalytic site.[34] We planned to introduce different electrophilic warheads on the right part of the bithiazole scaffold that would point towards LYS549 in the PI4KIIIβ ATP-binding pocket. Starting from compound **10**, easily prepared by refluxing **8** with thiourea, we introduced reactive electrophilic moieties on the free amino group by reaction with the proper acyl chloride (Scheme 1). First, by reaction with acryloyl chloride, we introduced an acrylamide Michael acceptor (compound **9e**), commonly found in many covalent kinase inhibitors. Following the same procedure and using propionyl chloride, we synthesized its unreactive saturated analogue (compound **9f**), to be used as a reference compound in the evaluation of the mechanism of action of these covalent inhibitors. Similarly we obtained the bromoacetamide derivative (**9g**) and we also added an isopropyl group to the terminal carbon of the acrylamide (**9h**) to reduce the electrophilic reactivity of the Michael acceptor. For the synthesis of compound **9h**, the acyl chloride was prepared in situ from the corresponding acid, synthesized following the procedure reported in literature.[35] Compound **9i** was obtained by reaction of **10** with the commercial 2-chloroethanesulfonyl chloride in the presence of an excess of base to generate the reactive vinyl sulfonamide Michael acceptor.[36]

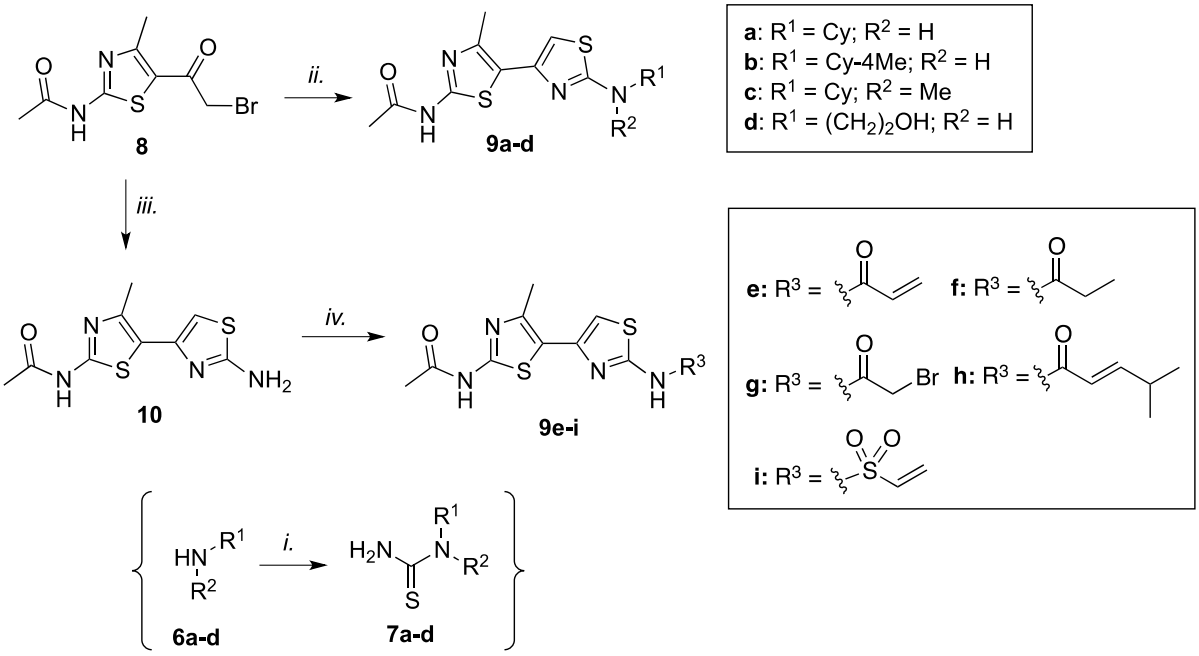

Scheme 1. Reagents and conditions: *i.* (a) benzoyl isothiocyanate, DCM, rt, 12 h, (b) method A (for **7a,b,d**) NaOH 1N, THF, reflux, 2-18 h, 80-85%, method B (for **7c**) N_2H_4 H_2O, rt, 3 h, 76%; *ii.* EtOH, reflux, 1 h, 75-95%; *iii.* thiourea, EtOH, reflux, 40 min, 90%; *iv.* (a) method A (for **9e-h**) R^3Cl, DIPEA, THF, rt, 2-6 h, 43-74%, method B (for **9i**) 2-chloroethanesulfonyl chloride, DIPEA, DMAP, THF, rt, 12 h, 40%.

Table 1. Activity of synthesized derivatives **9a-i** in PI4KIIIβ inhibition assay and in virus-cell-based enterovirus 71 (EV71) assay.

Cpd	PI4K IIIβ IC_{50} (μM)[a]			LLE from IC_{50} (PI4KIIIβ)	LELP from IC_{50} (PI4KIIIβ)	cLogP	EV71		
	t = 0 min	t = 5 min	t = 20 min				EC_{50} (μM)[a]	CC_{50} (μM)[b]	SI[c]
9a	8.29	-[d]	-	3.88	8.34	4.20	1.10 ± 0.16	25.50 ± 20.70	23.2
9b	14.16	-	-	3.38	9.55	4.47	0.34 ± 0.04	10.90	32.2
9c	9.52	-	-	3.57	9.31	4.45	0.88 ± 0.01	19.40 ± 2.08	22.1
9d	4.50	-	-	6.22	3.53	2.13	12.60 ± 0.02	333.00 ± 2.60	26.4
9e	2.16	0.57	0.14	5.86	4.90	2.97	1.89	6.01 ± 0.80	3.2

9f	5.39	5.58	5.21	5.18	5.52	3.16	NA	-	-
9g	2.11	1.71	1.67	5.57	5.17	3.06	NA	-	-
9h	17.40	4.84	5.58	3.72	8.72	4.03	107.00 ± 94.70	172.00 ± 8.25	1.6
9i	NA[e]	-	-	-	-	2.32	>290.00	-	-
1	0.48	-	-	4.90	8.60	4.40	0.92 ± 2.75	16.50 ± 9.04	17.9

[a]Values are the mean of at least three independent experiments. [b]CC_{50} values were assessed by MTS method. [c]Selectivity index (SI = CC_{50}/EC_{50}). [d]- = not determined. [e]NA = not active.

All the synthesized compounds were initially evaluated for their inhibitory potency against PI4KIIIβ kinase *in vitro* and for their cell-based antiviral activity against enterovirus 71 (EV71) using **1** as reference compound. As shown in Table 1, most compounds showed a low micromolar activity against PI4KIIIβ (column t = 0 min) while only compound **9i** was inactive. Compounds **9e-i** were also analyzed to confirm their irreversible inhibition of the PI4KIIIβ kinase using **9f** as a reference compound. For a reversible inhibitor, in a reaction mixture, an equilibrium of free enzyme and enzyme in complex with the inhibitor is established ([E] « [E:I]). As a result, once the equilibrium has been reached, the proportion of enzyme inhibited by the reversible inhibitor does not change over time. On the contrary, for an irreversible inhibitor, once the [E:I] complex has formed, dissociation of the enzyme cannot occur. The amount of [E:I] complex therefore increases over time. Assessing the potency of inhibitors at different time points, can thus allow us to discriminate between reversible and irreversible inhibitors. We performed inhibition assays leaving the enzyme in pre-incubation with the inhibitors for different times [0 min (no pre-incubation); 5 min; 20 min] (Table 1). As expected for a reversible inhibitor, the calculated IC_{50} of compound **9f** did not change over time. On the other hand, compounds **9e** and **9h** showed IC_{50} values that decreased with increasing time of pre-incubation. In particular for compound **9e**, the IC_{50} decreased by about 15 fold from 2.16 μM (with no pre-incubation) to 0.14 μM (after 20 minutes of pre-incubation). Similarly, the

IC_{50} value of **9h** decreased by about 3 fold after 20 minutes of pre-incubation with the enzyme. In contrast, the bromoacetamide derivative **9g** (with stable IC_{50} values in the same pre-incubation time frame) did not seem to exhibit a similar irreversible mechanism of action.

Cell-based antiviral activity of compounds **9a-i** was evaluated in an EV71-induced CPE-reduction assay in rhabdosarcoma (RD) cells. The EC_{50} and CC_{50} values allowed us to calculate the selectivity index (SI), defined as CC_{50}/EC_{50}. Compounds **9a-d** inhibited EV71 replication at low micromolar concentrations and with a good selectivity index (>20). However, the activity of compounds **9b,c** was associated with some morphological alterations of RD cells. On the other hand, both compounds **9a,d** showed a good antiviral profile and **9d** also had little effect on the uninfected host cells (minimal cytotoxicity). Compounds **9a-d** were also evaluated for their CFTR corrector activity using the pHTomato assay[37]: none of the compounds showed any effect on F508del-CFTR membrane exposure. Among compounds **9e-i**, only **9e** was able to inhibit EV71 replication at low micromolar concentration but this covalent PI4KIIIβ inhibitor had unacceptable levels of cytotoxicity and no further studies were conducted on these derivatives.

From this first round of evaluations, it was clear that the introduction of aliphatic moieties on the right portion of the bithiazole scaffold only resulted in a slight loss of affinity for PI4KIIIβ without a major decrease in antiviral activity (see Table 1). Interestingly, a free NH on the right side of the bithiazole is not needed for PI4KIIIβ inhibition and antiviral activity (Table 1, compound **9a** vs **9c**) and this observation reveals additional space for chemical exploration. Finally, an ethanolamine chain on the right resulted in a compound with very low cytotoxicity (**9d**), while the absence of CFTR corrector activity may be due to the low steric bulk on the left of the molecule (C2 acetamido moiety) in line with the previous trend reported in Figure 1.

Based on the above observations, we planned the synthesis of the new compounds reported in Schemes 2-4. First, we decided to evaluate the effect of an additional ethoxy chain on the two most interesting compounds reported in Table 1: the hit **1** and derivative **9a**. The secondary amines **11a,b** (the synthesis of **11a** is reported in the Supporting Info) were converted into the corresponding thioureas **12a,b** by reaction with ammonium thiocyanate (for **12a**) or benzoyl isothiocyanate followed by basic deprotection (for **12b**). The latter intermediates were then cyclized by reaction with intermediate **8** in refluxing ethanol to give the desired compounds **13a,b** in good yields (Scheme 2).

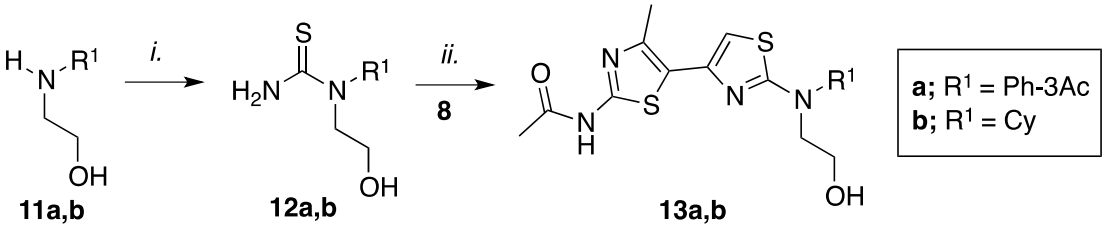

Scheme 2. Reagents and conditions: *i.* method A (for **12a**) NH_4SCN, HCl 1N, 100 °C 12 h, 65%, method B (for **12b**) (a) benzoyl isothiocyanate, THF, reflux, 25 min, (b) LiOH 1M, THF, reflux, 5 h, 69%; *ii.* **8**, EtOH, reflux, 1 h, 86-89%.

Next, we decided to modify compound **9d** (with low cytotoxicity) by introducing bulkier moieties on the left part of the bithiazole scaffold, in an attempt to increase CFTR correction efficacy as suggested by SAR analysis (Figure 1). The condensation of the intermediate **14**, previously prepared,[22] with the 1-(2-hydroxyethyl)thiourea **7d** gave the common intermediate **15**, whose hydroxyl group was then protected as *t*-butyldiphenylsilyl (TBDPS) ether (Scheme 3). The free 2-amino group on the 4-methylthiazole ring (left part) was then properly acylated by reaction with different acyl chlorides or anhydrides to obtain compounds **17a-c** after TBAF-deprotection of the crude mixture.

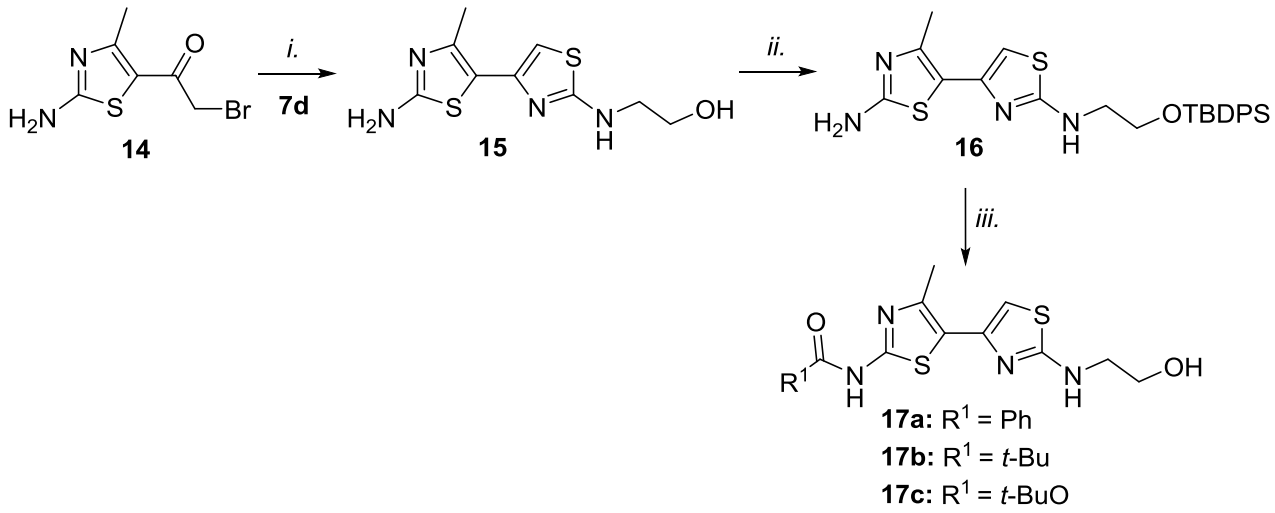

Scheme 3. *i.***7d**, EtOH, reflux, 1 h, 80%; *ii.* TBDPSCl, imidazole, CH_3CN, 0 °C, 30 min, 57%; *iii*. (a) R^1COCl (for **17a,b**) or di-*tert*-butyl dicarbonate (for **17c**), Et_3N, DCM, rt, 15 h; (b) TBAF 1.0 M in THF, CH_3COOH, THF, rt, 18 h, 60-77%.

Having previously selected the *tert*-butyl amide moiety as the best compromise between lipid kinase inhibition/selectivity and F508del-CFTR correction efficacy, we decided to modify compounds **13a,b** by introducing this bulkier group on the left part of the bithiazole scaffold. We also decided to introduce aromatic/aliphatic carboxy moieties on the right part of the molecule that may give profitable interactions with positively charged lysine residues (Lys549, Lys377) in the binding pocket. Intermediate **18**, previously prepared,[22] was reacted with pivaloyl chloride to give compound **19** which was then brominated in α to the carbonyl, thus providing the key intermediate **20**. The latter compound was finally cyclized by reaction with thioureas **12a,b** or **22a-f** (synthesis of **22a-f** in the Supp Inf) affording the expected compounds **23a-f** (Scheme 4).

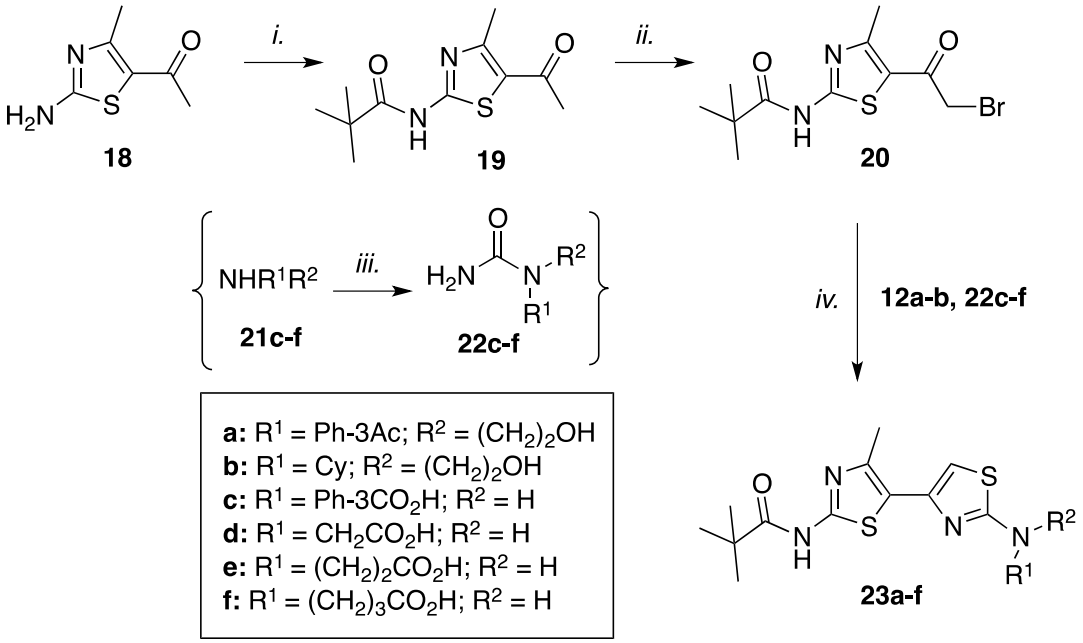

Scheme 4. Reagents and conditions: *i.* pivaloyl chloride, pyridine, THF, reflux, 12 h, 90%; *ii.* Br_2, 1,4-dioxane, 50 °C, 18 h, 80%; *iii*. method A (for **22c**) NH_4SCN, HCl 1N, 100 °C 12 h, 65%, method B (for **22d-f**) (a) $SOCl_2$, MeOH, reflux, 12 h, (b) benzoyl isothiocyanate, DCM, rt, 1 h, (c) NaOH 1M, MeOH, reflux, 2 h, 60-72%; *iv.* **12a,b**, **22c-f**, EtOH, reflux, 1h, 68-88%.

The second set of synthesized derivatives (compounds **13**, **17** and **23**) was also first assessed with respect to inhibitory potency against isolated PI4KIIIβ and antiviral activity against EV71. As shown in Table 2, all compounds inhibited PI4KIIIβ at micromolar and sub-micromolar concentrations with **13b**, **17b** and **23c** being the most potent kinase inhibitors *in vitro*. PI4KIIIβ inhibition correlates well with antiviral effect on EV71 replication with the notable exception of compounds **13b** and **17a**. Compounds endowed with the most promising inhibitory potency against EV71 and higher selectivity index (**13a**, **17b**, **23a**, **23c**) were also tested against additional EVs: coxsackievirus B3 (CVB3), rhinovirus group A (RV02), and rhinovirus group B (RV14). Results confirmed compounds **17b**, **23a** and **23c** as having the most promising antiviral activity against this panel of entero/rhinoviruses, while the hit compounds **1** and **2**

showed lower SI values in EV71 replication and no activity (**1**) or high toxicity (**2**) against hRV02 and hRV14.

Table 2. Activity of synthesized derivatives **13**, **17**, **23** in PI4KIIIβ inhibition assay and against a representative panel of Enteroviruses.

Cpd	PI4K IIIβ IC_{50} (μM)[a]	EV71			CVB3		hRV02		hRV14	
		EC_{50} (μM)[a]	CC_{50} (μM)[b]	SI[c]	EC_{50} (μM)[a]	CC_{50} (μM)[b]	EC_{50} (μM)[a]	CC_{50} (μM)[b]	EC_{50} (μM)[a]	CC_{50} (μM)[b]
13a	0.60	NA[c]	-[d]	-	-	-	-	-	-	-
13b	5.80	1.10 ± 0.86	16.40 ± 1.12	95.50	16.10	20.80	>263.00	>4.51	6.24	4.51 ± 0.52
17a	1.54	NA	-	-	-	-	-	-	-	-
17b	0.73	1.83 ± 0.32	361.00 ± 55.80	113.00	2.30	>293	5.40	41.20	3.80	41.20
17c	1.36	11.40 ± 1.30	>421	>37.60	-	-	-	-	-	-
23a	2.10	<0.43 (EC_{90} = 5.78)	28.90 ± 10.50	>67.20	6.60	>218	6.10	16.80	>9.1	16.80
23b	3.40	4.96 ± 1.85	4.46 ± 1.85	-	-	-	-	-	-	-
23c	0.09	0.42 ± 0.01	32.10 ± 8.10	53.90	17.00	110.70	9.70	36.30	15.30	36.30
23d	9.93	5.31 ± 0.26	>282	>54.5	-	-	-	-	-	-
23e	5.46	6.48 ± 1.88	>271	>33.1	-	-	-	-	-	-

23f	6.98	7.27 ± 0.82	261	38.8	-	-	-	-	-	-
1	0.48	0.92 ± 2.75	16.50 ± 9.04	17.90	2.17	101.00 ± 33.60	NA	-	NA	-
2	0.32	0.27 ± 0.50	7.94 ± 1.24	29.20	1.31	15.10	2.01 ± 0.05	4.07 ± 1.43	4.85 ± 1.09	3.87 ± 1.62

[a]Values are the mean of at least three independent experiments. [b]CC_{50} values were assessed by MTS method. [c]Selectivity index (SI = CC_{50}/EC_{50}). [d]- = not determined. [e]NA = not active.

Interestingly, the introduction of an ethoxy chain on the right side of the bithiazole scaffold was able to convert the relatively cytotoxic compound **2** into the less toxic and broad-spectrum antiviral compound **23a**.

Next, compounds **13**, **17** and **23** (reported in Table 2) were evaluated for their CFTR corrector/potentiator activity. As shown in Figure 2A, four compounds (**17b**, **23a-c**) acted as F508del-CFTR correctors, increasing steady-state levels of F508del-CFTR at the plasma membrane after 24 h incubation at 10 μM. Confirmatory tests on selected derivatives **17** and **23**, in comparison with hits **3** and **4**, were conducted at 3 μM concentration of each molecule. All compounds increased CFTR plasma membrane exposure (Figure 2B), with an effect that was comparable (for **23a**,**b**) to that of Lumacaftor (VX809). With the exception of compound **17b**, the improvement in CFTR biogenesis caused by all the other compounds also led to increased anion permeability, estimated from fluorescence quenching of a CFTR-fused YFP probe following extracellular iodide addition (Figure 2C).

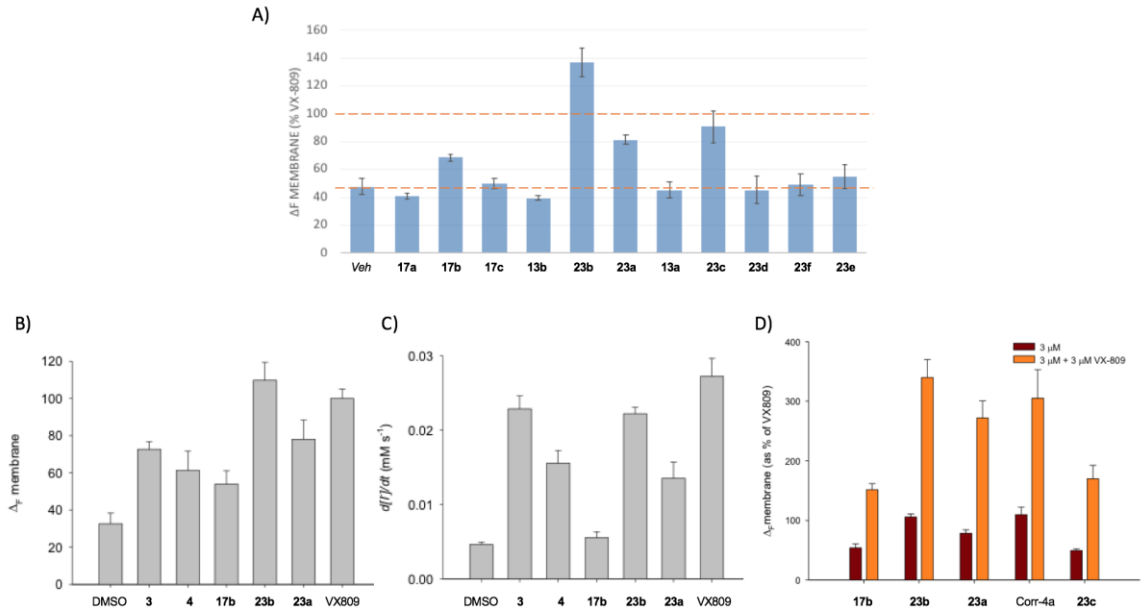

Figure 2. Effects of selected compounds on CFTR biogenesis and function. All treatments were carried out alongside low temperature incubation (30ºC), known to improve F508del-CFTR membrane localization, in order to increase the fluorescence signal. A) F508del-CFTR-pHTomato present at the plasma membrane was quantified following 24 h incubation in 10 μM of each drug. Incubation with VX809 (Lumacaftor) was assessed in parallel, as a positive control and results were reported as % of VX809 effect (Δ_F %). B) Same as in A conducted on selected compounds **17** and **23** incubated at 3 μM in comparison with hit molecules **3** and **4**. C) Anion permeability quantified using a YFP-F508del-CFTR probe[37] following 24 h treatment as in A. D) F508del-CFTR-pHTomato exposed at the plasma membrane, estimated following 24 h incubation with a lower concentration [3μM] of the indicated compounds, with or without VX-809.

The four most interesting derivatives, **17b**, **23a-c**, structural analogues of Corr-4a, can be considered as belonging to the so called Class II correctors[38] whose binding site on CFTR (still unknown) was shown to be distinct from that of Class I correctors (e.g. Lumacaftor, VX-809).[39,40] As mentioned in the introduction, combinations of correctors from different classes

are quite efficient in restoring F508del-CFTR functionality and here we evaluated the interaction between our best derivatives and VX-809, using the Corr-4a/VX-809 combination as reference (Figure 2D). All combinations showed an additive effect in improving F508del-CFTR membrane-localization and the best results were obtained with **23a**/VX809 and **23b**/VX-809 combinations, which improved the effect of VX-809 and increased the F508del-CFTR membrane density up to three fold higher than seen with VX-809 alone. This confirms that our dual-acting molecules, like Corr-4a, are likely to belong to the class-II family of correctors and target a binding site on the F508del-CFTR that is different from that targeted by VX-809.

To select the most suitable candidate for subsequent *in vivo* acute toxicity studies, a multi-dimensional SAR analysis was conducted by plotting the size-adjusted PI4KIIIβ activity (expressed as LELP), antiviral activity (expressed as EV71 EC_{50}), CFTR correction potency (expressed as F508del-CFTR membrane exposure) and cLogP for the synthesized multitarget inhibitors (**9a-i**, **13a-b**, **17a-c**, **23a-f**) with respect to those of previously reported hits (**1-4**) and reference compound **5** (Corr-4a) (Figure 3).

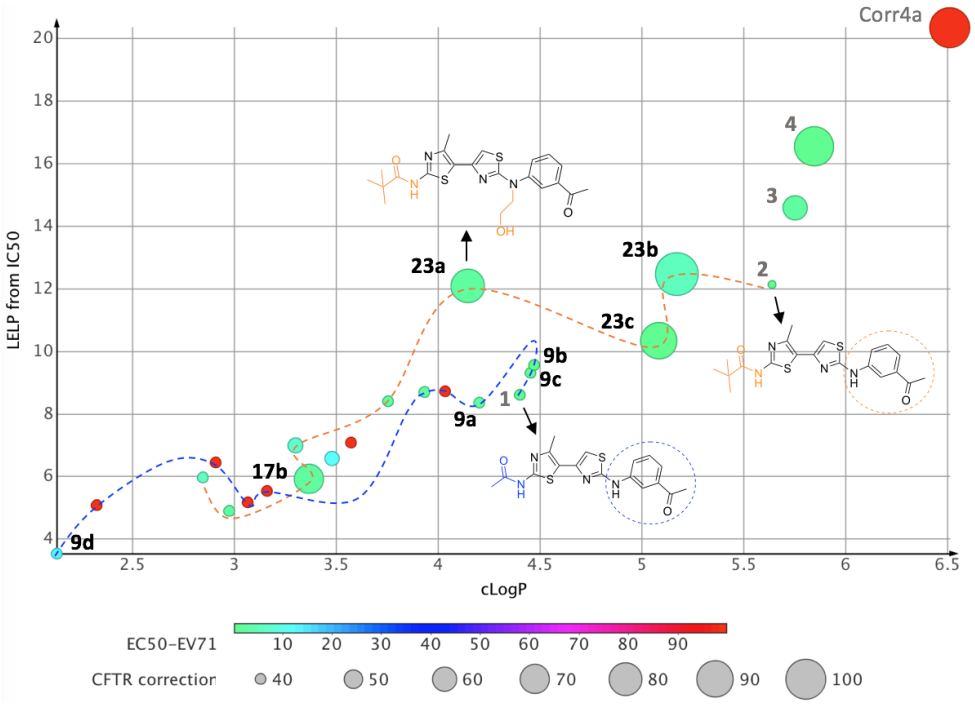

Figure 3. A scatter plot of LELP (based on PI4KIIIβ IC_{50}) versus cLogP for all synthesized and reference compounds. Colors represent EV71 antiviral activity. Size of the circles represents CFTR F508del-CFTR membrane exposure expressed as percentage of exposure obtained following VX-809 incubation. The most representative compounds are labelled. Dotted blue line follows the evolution of hit **1**. Dotted orange line follows the evolution of hit **2**. Plotted using Datawarrior.[32]

Lipophilicity-based metrics have been correlated to ADMET properties and may help identify those compounds endowed with favorable pharmacokinetic and safety properties (LELP <10) while looking at the most balanced multitarget activity profile. As we initially mentioned, hit compounds **1** and **2** were chosen as starting points for structure optimization (described by dotted lines in Figure 3) because of their better multitarget profile and LLE/LELP metrics compared to **3** and **4**, while Corr-4a is just a pure CFTR corrector with high lipophilicity. Starting from compound **1** and keeping the acetamido moiety on the left side of the molecule unchanged, structural modification on the right side (blue dotted circle) led to a series of derivatives (along the blue dotted line) with good LELP, comparable or lower lipophilicity than **1** and, in a few cases (**9a-d**), promising antiviral activity but no effect as CFTR correctors. On the other hand, starting from compound **2** and keeping the pivaloylamido moiety on the left side of the molecule unchanged, structural modification on the right side (orange dotted circle) led to a series of derivatives (along the orange dotted line) with a wide range of LELP, lower lipophilicity, good antiviral activity and, in a few cases (**17b**, **23a-c**) improved CFTR corrector properties. Among the latter four compounds, **17b** had the best profile in terms of PI4KIIIβ inhibition, broad-spectrum antiviral activity and LELP but it showed the lower F508del-CFTR correction potency and additivity but no synergy with VX809. Compound **23b** showed the best F508del-CFTR correction activity, some degree of

synergy with VX809, moderate PI4KIIIβ inhibition and antiviral activity but high cytotoxicity. Compound **23c** showed the best PI4KIIIβ inhibition potency and was relatively potent/selective against EV71, showed good F508del-CFTR correction potency but simple additivity with VX809 and borderline LELP. Compound **23a** showed moderate PI4KIIIβ inhibition potency and some interesting activity against EV71 and CVB3, good F508del-CFTR correction potency, additivity and possible synergy with VX809 plus borderline LELP with lower lipophilicity than **23c** and Corr-4a. Overall, the multitarget compound **23a** showed the most balanced activity profile and, despite its borderline LELP metrics, it was selected for acute toxicity studies *in vivo*.

Male C57BL/6 mice (8-12 weeks old) maintained under standard conditions (12:12h light-dark cycle, 22-24°C, food and water available ad libitum) and following 4 hours of fasting, were treated with **23a**, administered subcutaneously (s.c.) at 20, 60 and 180mg/kg (3 mice/dose). A battery of tests to evaluate physical appearance and changes in unprovoked and provoked behavior, motor activity, coordination and sensory/motor reflexes were carried out immediately before fasting, 1h and 24h after **23a** administration. Body weight was also assessed before and after fasting, prior to **23a** treatment, and daily thereafter for a total of 14 days. Results showed that **23a** was well tolerated at all the three tested doses: no changes in motor coordination and sensory/motor reflexes could be detected following doses up to 180mg/kg s.c. and no behavioural alterations were observed up to 15 days after **23a** administration (Table 3). After fasting, **23a**-treated mice recovered initial body weight almost as quickly as vehicle-treated mice. Based on a previous report on the biodistribution of fluorescent bithiazole correctors in mice,[41] we analyzed the effect of **23a** on the histology of key biodistribution organs: lung parenchyma, intestine mucosa and liver. At both the time points (1h and 24h) considered after **23a** administration, the histological analysis revealed a normal morphology of the lung and liver parenchyma and of the intestinal mucosa (Figure 4).

Table 3. Signs of acute toxicity detected 1h and 24h after **23a** 180mg/kg s.c. administration

Parameters observed	Observations	Observations
	1h	**24h**
Skin/fur	N.C[a]	N.C
Eyes and mucous membranes	N.C.	N.C.
Cardiac/Respiratory signs	N.C.	N.C.
Somato-motor activity and coordination	N.C.	N.C.
Behavioural pattern	N.C.	N.C.
Corneal reflex	N.C.	N.C.
Salivation	N.O.[b]	N.O.
Tremor	N.O.	N.O.
Convulsions	N.O.	N.O.
Lethargy	N.O.	N.O.
Sleep	N.O.	N.O.
Coma	N.O.	N.O.
Mortality	N.O.	N.O.

[a] N.C.: not changed. [b] N.O.: not observed

In the lung parenchyma, the alveolar microstructure was well maintained, with no sign of alveolar/interstitial inflammatory infiltrate nor haemorrhage in **23a** treated mice. In the airways, no alteration of the ciliated pseudo-stratified columnar epithelium, comprising ciliated cells, goblet and basal cells, was noted. The small intestine mucosa showed a normal columnar lining cell with regular distribution of Goblet cells, without signs of epithelial hyperplasia and inflammation of the submucosa. No morphological intestinal alteration was detected after **23a** treatment. In the liver, a normal hepatic labyrinth of hepatocytes aligning with the bile ductules was detected. The characteristic granular appearance of hepatocytes with varying amounts of

vacuolation and basophilic material, representing endoplasmic reticulum, was seen both in control and **23a**-treated animals at both experimental time points without morphological alterations. In summary, compound **23a** did not show severe citotoxicity *in vitro*, nor were any serious clinical signs observed in the acute toxicity study.

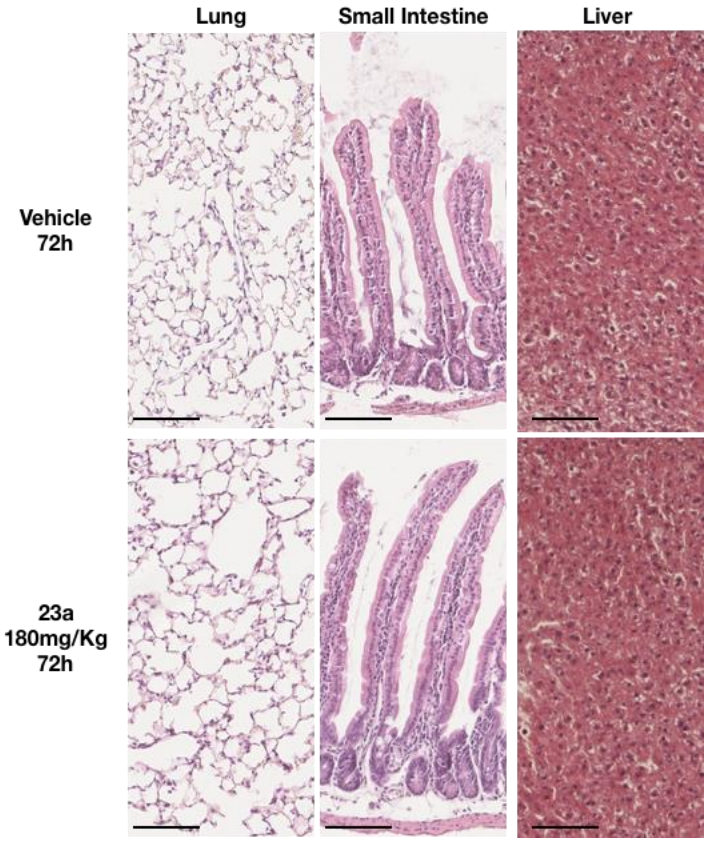

Figure 4. Representative Microphotographs of the lung, small intestine and liver of mice treated with the highest dose of compound **23a** and vehicle-treated mice. Scale bar 100 µm.

CONCLUSIONS

The simplification of therapeutic complexity and burden in CF care is one of the top ten priorities of future CF treatment. To address this issue, we have reported in this work the optimization of an original polypharmacology approach recently established by our group: the development of a well-balanced multitarget inhibitor able to simultaneously correct F508del-

CFTR and inhibit the replication of picornaviruses responsible of pulmonary exacerbation. Chemical exploration of the hit bithiazole scaffolds guided by multidimensional SAR allowed to identify a number of promising compounds able to inhibit PI4KIIIβ (and thus picornavirus replication), correct the F508del-CFTR folding defect and act additively with the class I corrector lumacaftor (VX-809). The most promising compound **23a** showed a well-balanced multitarget activity profile, inhibiting at low micromolar concentration PI4KIIIβ and selected picornaviruses (EV71, CVB3, hRV02), increasing steady-state levels of F508del-CFTR at the plasma membrane (around 80% of VX809 effect) and anion permeability (around 50% of VX-809 effect) and acting additively/synergically with VX-809 to increase F508del-CFTR membrane density up to three fold higher than VX-809 alone. Finally, *in vivo* acute toxicity studies showed that compound **23a** was well tolerated by C57BL/6 mice with no sign of toxicity and histological alterations in key biodistribution organs up to 180mg/kg. Compound **23a** represent therefore an excellent starting point to better understand the benefits and potentiality offered by a polypharmacology approach in comparison with standard CF treatments. Future efforts will be focused on further compounds' optimization and quantification of known PI4KIIIβ-mediated beneficial side effects, such as restoration of airway surface liquid (ASL) fluidity by indirectly downmodulating epithelial Na(+) channel (ENaC) and prevention of acute cellular rejection that may cause premature graft loss in CF patients who have received lung transplantation.

EXPERIMENTAL SECTION

Chemistry

General. All commercially available chemicals were purchased from both Sigma-Aldrich and Alfa Aesar and, unless otherwise noted, used without any previous purification. Solvents used for work-up and purification procedures were of technical grade. Dry solvents used in the

reactions were obtained by distillation of technical grade materials over appropriate dehydrating agents. Reactions were monitored by thin layer chromatography on silica gel-coated aluminium foils (silica gel on Al foils, SUPELCO Analytical, Sigma-Aldrich) at 254 and 365 nm. Where indicated, products were purified by silica gel flash chromatography on columns packed with Merck Geduran Si 60 (40-63 μm). ^{1}H and ^{13}C NMR spectra were recorded on BRUKER AVANCE 300 MHz and BRUKER AVANCE 400 MHz spectrometers. Chemical shifts (δ scale) are reported in parts per million relative to TMS. ^{1}H-NMR spectra are reported in this order: multiplicity and number of protons; signals were characterized as: *s* (singlet), *d* (doublet), *t* (triplet), *q* (quadruplet), *m* (multiplet), *bs* (broad signal). ESI-mass spectra were recorded on an API 150EX apparatus and are reported in the form of (m/z). Elemental analyses were performed on a Perkin-Elmer PE 2004 elemental analyzer. All final compounds showed chemical purity ≥95% as determined by elemental analysis data for C, H, and N (within 0.4% of the theoretical values). All final and reference compounds passed the PAINS filter.[42]

*General Procedure for the Synthesis of Compounds **9a-d**.* A solution of intermediate **8** (50 mg, 0.18 mmol) and the proper thiourea **7a-d** (0.18 mmol) in ethanol (2.5 mL) was heated at reflux for 1 h. After cooling to room temperature, saturated aqueous $NaHCO_3$ solution, H_2O and ethyl acetate were added and the aqueous phase was extracted three times with ethyl acetate. The combined organic phases were washed with brine, dried over Na_2SO_4 and evaporated. The crude was purified by flash chromatography using DCM/MeOH (from 97/3 to 95/5) as eluent.

*N-(2-(cyclohexylamino)-4'-methyl-[4,5'-bithiazol]-2'-yl)acetamide (**9a**).* Yield 90%. MS (ESI) $[M + H]^+$: 337.3 *m/z*. ^{1}H NMR (DMSO-d_6 300 MHz): δ 1.08-1.34 (m, 5H), 1.55-1.59 (m,

1H), 1.69-1.73 (m, 2H), 1.91-1.99 (m, 2H), 2.12 (s, 3H), 2.42 (s, 3H), 3.38-3.42 (m, 1H), 6.58 (s, 1H), 7.66 (d, 1H, *J* = 7.5 Hz), 11.98 (s, 1H). ^{13}C NMR (DMSO-d_6 100 MHz): δ 17.43, 22.91, 24.86 (2x), 25.78, 32.67 (2x), 53.99, 100.41, 121.13, 142.50, 143.29, 155.29, 167.52, 168.59. Anal. ($C_{15}H_{20}N_4OS_2$) C, H, N.

N-(4'-methyl-2-((4-methylcyclohexyl)amino)-[4,5'-bithiazol]-2'-yl)acetamide ***(9b)***. Yield 95%. MS (ESI) $[M + H]^+$: 351.3 *m/z*. ^{1}H NMR ($CDCl_3$ 400 MHz): δ 0.91 (d, 3H, *J* = 5.5 Hz), 1.04-1.10 (m, 2H), 1.19-1.22 (m, 2H), 1.25-1.27 (m, 2H), 1.74-1.77 (m, 2H), 2.12 (s, 3H), 2.17 (bs, 1H), 2.51 (s, 3H), 3.21 (bs, 1H), 6.00 (d, 1H, *J* = 7.1 Hz), 6.41 (s, 1H), 11.60 (s, 1H). ^{13}C NMR (DMSO-d_6 100 MHz): δ 17.00, 22.13, 22.94, 29.70, 31.91 (2x), 33.85 (2x), 55.65, 101.16, 121.54, 142.17, 143.30, 156.68, 168.21, 168.79. Anal. ($C_{16}H_{22}N_4OS_2$) C, H, N.

*N-(2-(cyclohexyl(methyl)amino)-4'-methyl-[4,5'-bithiazol]-2'-yl)acetamide (**9c**).*

Yield 93%. MS (ESI) $[M + H]^+$: 351.0 *m/z*. ^{1}H NMR ($CDCl_3$ 400 MHz): δ 1.12-1.18 (m, 1H), 1.37-1.54 (m, 4H), 1.69-1.72 (m, 1H), 1.85-1.87 (m, 4H), 2.23 (s, 3H), 2.58 (s, 3H), 3.00 (s, 3H), 3.81 (bs, 1H), 6.42 (s, 1H), 11.74 (s, 1H). ^{13}C NMR ($CDCl_3$ 100 MHz): δ 17.18, 23.16, 25.57, 25.85 (2x), 29.83 (2x), 32.16, 60.24, 100.55, 122.42, 141.71, 143.91, 156.96, 168.09, 169.99. Anal. ($C_{16}H_{22}N_4OS_2$) C, H, N.

*N-(2-((2-hydroxyethyl)amino)-4'-methyl-[4,5'-bithiazol]-2'-yl)acetamide (**9d**).* Yield 75%. MS (ESI) $[M + H]^+$: 299.2 *m/z*. ^{1}H NMR (DMSO-d_6 300 MHz): δ 2.12 (s, 3H), 2.42 (s, 3H), 3.31 (q, 2H, *J* = 5.7 Hz), 3.57 (t, 2H, *J* = 5.7 Hz), 4.76 (bs, 1H), 6.60 (s, 1H), 7.71 (t, 1H, *J* = 5.7 Hz), 11.97 (s, 1H). ^{13}C NMR (DMSO-d_6 100 MHz): δ 17.45, 22.92, 47.65, 59.90, 100.80, 121.08, 142.55, 143.16, 155.31, 168.55, 168.63. Anal. ($C_{11}H_{14}N_4O_2S_2$) C, H, N.

*Synthesis of N-(2-amino-4'-methyl-[4,5'-bithiazol]-2'-yl)acetamide (**10**).* A mixture of intermediate **8** (500 mg, 1.80 mmol) and thiourea (137 mg, 1.80 mmol) in ethanol (8.5 mL) was heated at reflux for 40 minutes. Then saturated aqueous $NaHCO_3$ solution and ethyl acetate were added to the mixture and the aqueous phase was extracted three times with ethyl acetate. The combined organic phases were washed with brine, dried over Na_2SO_4 and concentrated under vacuum. Compound **10** was used in the following step without any further purification. Yield 90%. MS (ESI) $[M + H]^+$: 255.2 *m/z*. ^{1}H NMR (DMSO-d_6 400 MHz): δ 2.11 (s, 3H), 2.41 (s, 3H), 6.56 (s, 1H), 7.12 (s, 2H), 11.96 (s, 1H).

*General Procedure for the Synthesis of Compounds **9e-h**.* DIPEA (46 μL, 0.29 mmol) was added to a stirred solution of intermediate **10** (50 mg, 0.20 mmol) in dry THF (2 mL) cooled to 0 °C. After 15 minutes a solution of the proper acyl chloride (0.29 mmol) in dry THF (0.5 mL) was added dropwise. The resulting solution was warmed to room temperature and stirred for 2-6 h, after which H_2O and ethyl acetate were added and the aqueous phase was extracted twice with ethyl acetate. The combined organic phases were washed with brine, dried over Na_2SO_4 and evaporated. The crude was purified by flash chromatography using DCM/MeOH (from 98/2 to 96/4) as eluent to give compounds **9e-h** as white solids.

*N-(2'-acetamido-4'-methyl-[4,5'-bithiazol]-2-yl)acrylamide (**9e**).* Yield 43%. MS (ESI) $[M + H]^+$: 309.2 *m/z*. ^{1}H NMR (DMSO-d_6 400 MHz): δ 2.14 (s, 3H), 2.48 (s, 3H), 5.91 (d, 1H, J = 10.0 Hz), 6.41 (d, 1H, J = 17.1 Hz), 6.55 (dd, 1H, J = 17.1, 10.0 Hz), 7.26 (s, 1H), 12.08 (s, 1H), 12.51 (s, 1H). ^{13}C NMR (DMSO-d_6 100 MHz): δ 17.41, 22.89, 108.52, 120.27, 129.80, 130.09, 142.49, 143.40, 155.82, 157.91, 163.52, 168.85. Anal. ($C_{12}H_{12}N_4O_2S_2$) C, H, N.

*N-(2'-acetamido-4'-methyl-[4,5'-bithiazol]-2-yl)propionamide (**9f**).* Yield 74%. MS (ESI) $[M + H]^+$: 311.4 *m/z*. ^{1}H NMR (DMSO-d_6 400 MHz): δ 1.10 (t, 3H, J = 7.5 Hz) 2.14 (s, 3H), 2.45

(q, 2H, *J* = 7.5 Hz), 2.47 (s, 3H), 7.19 (s, 1H), 12.06 (s, 1H), 12.22 (s, 1H). ^{13}C NMR (DMSO-d_6 100 MHz): δ 9.55, 17.40, 22.89, 28.66, 107.71, 120.42, 142.10, 143.23, 155.77, 158.07, 168.77, 172.76. Anal. ($C_{12}H_{14}N_4O_2S_2$) C, H, N.

*N-(2'-acetamido-4'-methyl-[4,5'-bithiazol]-2-yl)-2-bromoacetamide (**9g**).* Yield 68%. MS (ESI) $[M + H]^+$: 375.2 *m/z*. ^{1}H NMR (DMSO-d_6 400 MHz): δ 2.14 (s, 3H), 2.48 (s, 3H), 4.41 (s, 2H), 7.28 (s, 1H), 12.08 (s, 1H), 12.67 (s, 1H). ^{13}C NMR (DMSO-d_6 100 MHz): δ 17.36, 22.88, 42.71, 108.53, 120.13, 142.41, 143.55, 155.85, 157.54, 165.65, 168.96. Anal. ($C_{11}H_{11}BrN_4O_2S_2$) C, H, N.

*(E)-N-(2'-acetamido-4'-methyl-[4,5'-bithiazol]-2-yl)-4-methylpent-2-enamide (**9h**).* Yield 49%. MS (ESI) $[M + H]^+$: 351.4 *m/z*. ^{1}H NMR (DMSO-d_6 400 MHz): δ 1.05 (d, 6H, *J* = 6.7 Hz), 2.13 (s, 3H), 2.47 (s, 3H), 2.52-2.51 (m, 1H), 6.20 (d, 1H, *J* = 15.5), 6.96 (dd, 1H, *J* = 15.5, 6.7 Hz), 7.23 (s, 1H), 12.09 (s, 1H), 12.36 (s, 1H). ^{13}C NMR (DMSO-d_6 100 MHz): δ 17.40, 21.58 (2x), 22.89, 30.85, 108.26, 119.99, 120.37, 142.39, 143.31, 154.24, 155.79, 158.15, 164.02, 168.78. Anal. ($C_{15}H_{18}N_4O_2S_2$) C, H, N.

*Synthesis of N-(4'-methyl-2-(vinylsulfonamido)-[4,5'-bithiazol]-2'-yl)acetamide (**9i**).* DIPEA (105 µL, 0.60 mmol) and catalytic DMAP (2.4 mg, 0.02 mmol) were added to a stirred solution of intermediate **10** (50 mg, 0.20 mmol) in dry THF (4 mL). The mixture was cooled to 0 °C and a solution of 2-chloroethanesulfonyl chloride (30 µL, 0.29 mmol) in dry THF (0.5 mL) was added dropwise. The mixture was stirred at room temperature for 12 hours, after which H_2O and ethyl acetate were added and the aqueous phase was extracted twice with ethyl acetate. The combined organic phases were washed with saturated aqueous NH_4Cl solution, dried over Na_2SO_4 and evaporated. The crude was purified by flash chromatography using DCM/MeOH

(96/4) as eluent. White solid. Yield: 40%. MS (ESI) $[M + H]^+$: 345.2 *m/z*. ^{1}H NMR (DMSO-d_6 300 MHz): δ 2.14 (s, 3H), 2.21 (s, 3H), 5.96 (d, 1H, J = 16.8 Hz), 6.03 (d, 1H, J = 10.3 Hz), 6.89 (dd, 1H, J = 16.8, 10.3 Hz), 8.10 (s, 1H), 8.11 (s, 1H), 12.16 (s, 1H). ^{13}C NMR (DMSO-d_6 100 MHz): δ 17.11, 22.88, 115.35, 117.46, 127.32, 139.22, 147.96, 149.71, 157.63, 169.06, 171.17. Anal. ($C_{11}H_{12}N_4O_3S_3$) C, H, N.

*Synthesis of 1-(3-acetylphenyl)-1-(2-hydroxyethyl)thiourea (**12a**).* NH_4SCN (339 mg, 4.46 mmol) was added portionwise to a solution of amine **11a** (400 mg, 2.23 mmol) in HCl 1N (3 mL) and the mixture was heated at 100 °C for 12 h. After cooling to room temperature saturated aqueous $NaHCO_3$ solution and ethyl acetate were added to the mixture and the aqueous phase was extracted three times with ethyl acetate. The combined organic phases were washed with brine, dried over Na_2SO_4 and concentrated under vacuum. The crude was purified by flash chromatography using petroleum ether/ethyl acetate (3/7) as eluent. Yield 65%. MS (ESI) $[M + H]^+$: 239.2 *m/z*. ^{1}H NMR ($CDCl_3$ 400 MHz): δ 2.63 (s, 3H), 3.88 (t, 2H, J = 6.0 Hz), 4.38 (t, 2H, J = 6.0 Hz), 4.70 (bs, 1H), 5.90 (bs, 2H), 7.58 (d, 1H, J = 7.8 Hz), 7.61 (t, 1H, J = 7.8 Hz), 7.92 (s, 1H), 8.00 (d, 1H, J = 7.8 Hz).

*Synthesis of 1-cyclohexyl-1-(2-hydroxyethyl)thiourea (**12b**).* Benzoyl isothiocyanate (469 µL, 3.49 mmol) was added dropwise to a solution of *N*-ethylcyclohexylamine **11b** (500 mg, 3.49 mmol) in dry THF (9 mL) and the mixture was refluxed for 25 minutes. The solvent of reaction was evaporated, the residue was dissolved in THF/LiOH 1M (1/1, 15 mL) and the mixture was refluxed for 5 h. After cooling to room temperature, H_2O and ethyl acetate were added and the aqueous phase was extracted twice with ethyl acetate. The combined organic phases were dried over Na_2SO_4 and evaporated. The crude was purified by flash chromatography using petroleum ether/ethyl acetate (3/7) as eluent. Yield 69%. MS (ESI) [M

+ H]$^+$: 203.1 *m/z*. ^{1}H NMR (DMSO-d_6 300 MHz): δ 1.27-1.45 (m, 4H), 1.68-1.94 (m, 6H), 3.50 (m, 2H), 3.52 (bs, 1H), 3.87 (m, 2H), 5.03 (bs, 1H), 6.67 (bs, 2H).

*General Procedure for the Synthesis of Compounds **13a,b***. A solution of intermediate **8** (100 mg, 0.36 mmol) and the proper thiourea **12a,b** (0.36 mmol) in ethanol (2.5 mL) was heated at reflux for 1 h. After cooling down to room temperature, saturated aqueous $NaHCO_3$ solution, H_2O and ethyl acetate were added and the aqueous phase was extracted three times with ethyl acetate. The combined organic phases were washed with brine, dried over Na_2SO_4 and concentrated under vacuum. The crude was purified by flash chromatography using DCM/MeOH (96/4) as eluent, to give compounds **13a,b** as white solids.

*N-(2-((3-acetylphenyl)(2-hydroxyethyl)amino)-4'-methyl-[4,5'-bithiazol]-2'-yl)acetamide **(13a)***. Yield 86%. MS (ESI) [M + H]$^+$: 417.3 *m/z*. ^{1}H NMR (DMSO-d_6 300 MHz): δ 2.13 (s, 3H), 2.44 (s, 3H), 2.61 (s, 3H), 3.72 (q, 2H, *J* = 5.4 Hz), 4.03 (t, 2H, *J* = 5.4 Hz), 4.92 (t, 1H, *J* = 5.4 Hz), 6.76 (s, 1H), 7.63 (t, 1H, *J* = 7.8 Hz), 7.83 (d, 1H, *J* = 7.8 Hz), 7.90 (d, 1H, *J* = 7.8 Hz), 8.15 (s, 1H), 12.03 (s, 1H). ^{13}C NMR (DMSO-d_6 100 MHz): δ 17.40, 22.92, 27.31, 55.78, 58.26, 102.87, 120.51, 126.54, 126.98, 130.70, 131.61, 138.80, 143.18, 143.74, 145.86, 155.53, 168.65, 168.69, 197.82. Anal. ($C_{19}H_{20}N_4O_3S_2$) C, H, N.

*N-(2-(cyclohexyl(2-hydroxyethyl)amino)-4'-methyl-[4,5'-bithiazol]-2'-yl)acetamide **(13b)***. Yield 89%. MS (ESI) [M + H]$^+$: 381.4 *m/z*. ^{1}H NMR (DMSO-d_6 300 MHz): δ 1.12-1.34 (m, 3H), 1.56-1.64 (m, 3H), 1.79-1.82 (m, 4H), 2.12 (s, 3H), 2.44 (s, 3H), 3.40-3.41 (m, 2H), 3.58-3.60 (m, 3H), 4.83 (t, 1H, *J* = 5.4 Hz), 6.71 (s, 1H), 12.00 (s, 1H). ^{13}C NMR (DMSO-d_6 100 MHz): δ 17.39, 22.92, 25.47, 26.02 (2x), 30.30 (2x), 49.53, 59.33, 61.17, 100.91, 120.89, 142.84, 143.77, 155.36, 168.60, 169.14. Anal. ($C_{17}H_{24}N_4O_2S_2$) C, H, N.

*Synthesis of 2-((2'-amino-4'-methyl-[4,5'-bithiazol]-2-yl)amino)ethanol (**15**).* A mixture of intermediates **7d** (513 mg, 4.27 mmol) and **14** (1000 mg, 4.27 mmol) in ethanol (15 mL) was heated at reflux for 1 h. Then saturated aqueous $NaHCO_3$ solution and ethyl acetate were added to the mixture and the aqueous phase was extracted three times with ethyl acetate. The combined organic phases were washed with brine, dried over Na_2SO_4 and concentrated under vacuum. Ether was added to the crude and the solid obtained was filtered over a Buchner funnel, washed with ether and used in the following step without any further purification. Yield 80%. MS (ESI) $[M + H]^+$: 257.1 *m/z*. ^1H NMR (DMSO-d_6 300 MHz): δ 2.40 (s, 3H), 3.28 (q, 2H, J = 5.7 Hz), 3.47 (t, 2H, J = 5.7 Hz), 4.80 (bs, 1H), 6.60 (s, 1H), 7.75 (t, 1H, J = 5.7 Hz), 8.29 (s, 2H).

*Synthesis of N2-(2-((tert-butyldiphenylsilyl)oxy)ethyl)-4'-methyl-[4,5'-bithiazole]-2,2'-diamine (**16**).* *Tert*-butylchlorodiphenylsilane (946 µL, 3.69 mmol) was added dropwise to a cooled solution of intermediate **15** (860 mg, 3.35 mmol) and imidazole (456 mg, 6.70 mmol) in dry CH_3CN (7.5 mL). After stirring 30 minutes at 0 °C, saturated aqueous NH_4Cl solution and ethyl acetate were added to the mixture and the aqueous phase was extracted three times with ethyl acetate. The combined organic phases were washed with brine, dried over Na_2SO_4 and concentrated under vacuum. The crude was purified by flash chromatography using DCM/MeOH (95/5) as eluent. Yield 57%. MS (ESI) $[M + H]^+$: 495.2 *m/z*. ^1H NMR (DMSO-d_6 400 MHz): δ 0.99 (s, 9H), 2.24 (s, 3H), 3.48 (q, 2H, J = 5.6 Hz), 3.79 (t, 2H, J = 5.6 Hz), 6.32 (s, 1H), 6.88 (s, 2H), 7.39-7.47 (m, 7H), 7.57-7.73 (m, 4H).

*General Procedure for the Synthesis of Compounds **17a-c**.* Et_3N (56 µL, 0.40 mmol) was added to a stirred suspension of intermediate **16** (100 mg, 0.20 mmol) in dry DCM (4 mL) at 0 °C.

After 15 minutes a solution of the proper acyl chloride or anhydride (0.30 mmol) in dry DCM (0.5 mL) was added dropwise. The resulting solution was warmed to room temperature and stirred for 15 h. Next, H_2O and DCM were added and the aqueous phase was extracted twice with DCM. The combined organic phases were washed with brine, dried over Na_2SO_4 and evaporated. The residue was suspended in THF (3.5 mL), cooled to 0 °C and acetic acid (106 µL, 1.86 mmol) was added. Tetra-*n*-butylammonium fluoride (1.0 M solution in THF, 500 µL, 1.72 mmol) was added dropwise and the solution was warmed to room temperature and stirred for 18 h. Saturated aqueous NH_4Cl solution and ethyl acetate were added to the mixture and the aqueous phase was extracted three times with ethyl acetate. The combined organic phases were washed with brine, dried over Na_2SO_4 and concentrated under vacuum. The crude was purified by flash chromatography using DCM/MeOH (96/4) as eluent, affording compounds **17a-c** as white solids.

N-(2-((2-hydroxyethyl)amino)-4'-methyl-[4,5'-bithiazol]-2'-yl)benzamide ***(17a)***. Yield 70%. MS (ESI) $[M + H]^+$: 361.0 *m/z*. ^{1}H NMR (DMSO-d_6 400 MHz): δ 2.50 (s, 3H), 3.34-3.36 (m, 2H), 3.59 (q, 2H, J = 5.6 Hz), 4.78 (t, 1H, J = 5.6 Hz), 6.66 (s, 1H), 7.55 (t, 2H, J = 7.6 Hz), 7.64 (t, 1H, J = 7.6 Hz), 7.75 (t, 1H, J = 5.6 Hz), 8.10 (d, 2H, J = 7.6 Hz), 12.55 (s, 1H). ^{13}C NMR (DMSO-d_6 100 MHz): δ 17.28, 47.65, 59.92, 101.15, 121.55, 128.55 (2x), 129.06 (2x), 132.65, 132.98, 142.80, 143.04, 155.31, 165.46, 168.60. Anal. ($C_{16}H_{16}N_4O_2S_2$) C, H, N.

N-(2-((2-hydroxyethyl)amino)-4'-methyl-[4,5'-bithiazol]-2'-yl)pivalamide ***(17b)***. Yield 77%. MS (ESI) $[M + H]^+$: 341.3 *m/z*. ^{1}H NMR (DMSO-d_6 400 MHz): δ 1.23 (s, 9H), 2.50 (s, 3H), 3.31-3.33 (m, 2H), 3.57-3.58 (m, 2H), 4.77 (bs, 1H), 6.59 (s, 1H), 7.72 (t, 1H, J = 5.6 Hz), 11.65 (s, 1H). ^{13}C NMR (DMSO-d_6 100 MHz): δ 17.33, 27.09 (3x), 39.14, 47.63, 59.89, 100.75, 121.15, 142.47, 143.22, 156.04, 168.51, 176.91. Anal. ($C_{14}H_{20}N_4O_2S_2$) C, H, N.

*tert-butyl (2-((2-hydroxyethyl)amino)-4'-methyl-[4,5'-bithiazol]-2'-yl)carbamate (**17c**).* Yield 60%. MS (ESI) $[M + H]^+$: 357.2 *m/z*. ^{1}H NMR (DMSO-d_6 400 MHz): δ 1.48 (s, 9H), 2.39 (s, 3H), 3.31-3.33 (m, 2H), 3.56-3.58 (m, 2H), 4.78 (bs, 1H), 6.56 (s, 1H), 7.72 (bs, 1H), 11.33 (s, 1H). ^{13}C NMR (DMSO-d_6 100 MHz): δ 17.37, 28.37 (3x), 47.50, 59.90, 81.52, 100.48, 120.86, 142.85, 143.09, 157.03, 168.39, 172.11. Anal. ($C_{14}H_{20}N_4O_3S_2$) C, H, N.

*Synthesis of N-(5-acetyl-4-methylthiazol-2-yl)pivalamide (**19**).* Intermediate **18** (1000 mg, 6.40 mmol) was suspended in dry THF (12 mL) and the mixture was cooled to 0 °C. Pyridine (1.3 mL) was added, followed by the dropwise addition of pivaloyl chloride (1.18 mL, 9.60 mmol). The reaction mixture was allowed to warm to room temperature and heated at reflux for 12 hours. Next, H_2O and ethyl acetate were added and the aqueous phase was extracted three times with ethyl acetate. The combined organic phases were washed three times with saturated aqueous NH_4Cl solution and brine, dried over Na_2SO_4 and concentrated under vacuum. Compound **19** was used in the next step without any further purification. Yield: 90%. MS (ESI) $[M + H]^+$: 241.4 *m/z*. ^{1}H NMR (DMSO-*d6* 400 MHz): δ 1.19 (s, 9H), 2.47 (s, 3H), 2.58 (s, 3H), 12.16 (s, 1H).

*Synthesis of N-(5-(2-bromoacetyl)-4-methylthiazol-2-yl)pivalamide (**20**).*A solution of Br_2 (213 µL, 4.16 mmol) in 1,4-dioxane (4.7 mL) was added dropwise to a stirred solution of intermediate **19** (800 mg, 3.33 mmol) in 1,4-dioxane (12.7 mL). The mixture was heated at 50 °C for 18 h. After cooling down to room temperature, saturated aqueous $NaHCO_3$ solution and ethyl acetate were added and the aqueous phase was extracted three times with ethyl acetate. The combined organic phases were washed with brine, dried over Na_2SO_4 and concentrated under vacuum. The crude was purified by flash chromatography using petroleum ether/ethyl

acetate (8/2) as eluent. Yield 80%. MS (ESI) $[M + H]^+$: 319.3 *m/z*. ^{1}H NMR (DMSO-d_6 400 MHz): δ 1.24 (s, 9H), 2.60 (s, 3H), 4.64 (s, 2H), 12.32 (s, 1H).

*General Procedure for the Synthesis of Compounds **23a-f***. A solution of intermediate **20**(100 mg, 0.36 mmol) and the proper thiourea **12a,b** or **22c-f** (0.36 mmol) in ethanol (2.5 mL) was heated at reflux for 1 h. After cooling down to room temperature, saturated aqueous $NaHCO_3$ solution, H_2O and ethyl acetate were added and the aqueous phase was extracted three times with ethyl acetate. The combined organic phases were washed with brine, dried over Na_2SO_4 and concentrated under vacuum. The crude was purified by flash chromatography using DCM/MeOH (from 97/3 to 90/10) as eluent affording **23a-f** as white solids.

*N-(2-((3-acetylphenyl)(2-hydroxyethyl)amino)-4'-methyl-[4,5'-bithiazol]-2'yl)pivalamide **(23a)***. Yield 88%. MS (ESI) $[M + H]^+$: 459.3 *m/z*. ^{1}H NMR (DMSO-d_6 400 MHz): δ 1.30 (s, 9H), 2.45 (s, 3H), 2.59 (s, 3H), 3.96 (m, 2H), 4.15 (t, 2H, J = 5.8 Hz), 4.92 (bs, 1H), 6.76 (s, 1H), 7.63 (t, 1H, J = 7.8 Hz), 7.83 (d, 1H, J = 7.8 Hz), 7.90 (d, 1H, J = 7.8 Hz), 8.15 (s, 1H), 11.73 (s, 1H). ^{13}C NMR ($CDCl_3$ 100 MHz): δ 16.95, 26.74, 27.16 (3x), 39.08, 56.32, 61.50, 102.80, 121.37, 126.43, 127.16, 130.46, 131.38, 139.01, 142.87, 143.52, 145.93, 155.61, 169.90, 176.00, 197.18. Anal. ($C_{22}H_{26}N_4O_3S_2$) C, H, N.

*N-(2-(cyclohexyl(2-hydroxyethyl)amino)-4'-methyl-[4,5'-bithiazol]-2'-yl)pivalamide **(23b)***. Yield: 75%. MS (ESI) $[M + H]^+$: 423.5 *m/z*. ^{1}H NMR ($CDCl_3$ 300 MHz): δ 1.11-1.19 (m, 3H), 1.21 (s, 9H), 1.23-1.56 (m, 3H), 1.85-2.04 (m, 4H), 2.48 (s, 3H), 3.35-3.38 (m, 1H), 3.63-3.65 (m, 2H), 3.84-3.86 (m, 2H), 4.61 (bs, 1H), 6.40 (s, 1H), 8.99 (s, 1H). ^{13}C NMR ($CDCl_3$ 100 MHz): δ 16.90, 25.36, 25.86 (2x), 27.15 (3x), 30.59 (2x), 39.07, 48.50, 62.63, 63.96, 100.85, 121.54, 142.69, 143.34, 155.56, 171.11, 175.99. Anal. ($C_{20}H_{30}N_4O_2S_2$) C, H, N.

*3-((4'-methyl-2'-pivalamido-[4,5'-bithiazol]-2-yl)amino)benzoic acid (**23c**).*Yield: 68%. MS (ESI) [M - H]$^-$: 415.2 *m/z*. ^{1}H NMR (DMSO-d_6 400 MHz): δ 1.25 (s, 9H), 2.50 (s, 3H), 6.93 (s, 1H), 7.47 (t, 1H, *J* = 7.9 Hz), 7.54 (d, 1H, *J* = 7.9 Hz), 7.97 (d, 1H, *J* = 7.9 Hz), 8.24 (s, 1H), 10.50 (s, 1H), 11.75 (s, 1H), 11.80 (s, 1H). ^{13}C NMR (DMSO-d_6 100 MHz): δ 17.41, 27.08 (3x), 39.24, 103.56, 118.06, 120.37, 121.20, 122.53, 129.72, 132.05, 141.67, 143.40, 156.21, 163.07, 167.71, 168.01, 177.00. Anal. ($C_{19}H_{20}N_4O_3S_2$) C, H, N.

*2-((4'-methyl-2'-pivalamido-[4,5'-bithiazol]-2-yl)amino)acetic acid (**23d**).* Yield: 75%. MS (ESI) [M - H]$^-$: 353.2 *m/z*. ^{1}H NMR (DMSO-d*6* 400 MHz): δ 1.23 (s, 9H), 2.44 (s, 3H), 3.71 (d, 2H, *J* = 3.6 Hz), 6.59 (s, 1H), 7.44 (bs, 1H), 11.68 (s, 1H), 12.56 (bs, 1H). ^{13}C NMR (DMSO-d*6* 100 MHz): δ 17.34, 27.09 (3x), 39.08, 42.69, 100.95, 121.19, 142.41, 143.22, 156.02, 168.18, 173.61, 176.61. Anal. ($C_{14}H_{18}N_4O_3S_2$) C, H, N.

*3-((4'-methyl-2'-pivalamido-[4,5'-bithiazol]-2-yl)amino)propanoic acid (**23e**).* Yield: 87%. MS (ESI) [M - H]$^-$: 367.1 *m/z*. ^{1}H NMR (DMSO-d_6 400 MHz): δ 1.24 (s, 9H), 2.45 (s, 3H), 2.58 (t, 2H, *J* = 6.8 Hz), 3.43-3.47 (m, 2H), 6.62 (s, 1H), 7.78 (bs, 1H), 11.66 (s, 1H), 12.14 (s, 1H). ^{13}C NMR (DMSO-d_6 100 MHz): δ 17.34, 27.09 (3x), 31.67, 39.16, 45.35, 101.05, 121.22, 142.56, 143.12, 156.44, 168.18, 173.51, 176.09. Anal. ($C_{15}H_{20}N_4O_3S_2$) C, H, N.

*4-((4'-methyl-2'-pivalamido-[4,5'-bithiazol]-2-yl)amino)butanoic acid (**23f**).*Yield: 70%. MS (ESI) [M - H]$^-$: 381.1 *m/z*. ^{1}H NMR (DMSO-d_6 400 MHz): δ 1.24 (s, 9H), 1.77-1.84 (m, 2H), 2.31 (t, 2H, *J* = 7.4 Hz), 2.48 (s, 3H), 3.22-3.27 (m, 2H), 6.61 (s, 1H), 7.76 (t, 1H, *J* = 5.2 Hz), 11.68 (s, 1H), 12.08 (s, 1H). ^{13}C NMR (DMSO-d_6 100 MHz): δ 17.34, 24.56, 27.09 (3x), 31.54,

39.18, 44.34, 100.73, 121.12, 142.52, 143.39, 156.06, 168.40, 174.67, 176.89. Anal. ($C_{16}H_{22}N_4O_3S_2$) C, H, N.

Biology

In vitro kinase inhibition assays

Recombinant full length, HIS6-tagged PI4KIIIβ was purchased from ProQinase (Germany).

Assay conditions:

PI4KIIIβ reactions were performed in 10 µL using 20 mM Tris-HCl pH 7.5, 0.125 mM EGTA, 2 mM DTT, 0.04% Triton, 3 mM $MgCl_2$, 3 mM $MnCl_2$, 20 µM ATP, 0.01 µCi γ-P33 ATP, 200 µM Pi:3PS, 10% DMSO, 0.4 ng/µL of PI4KIIIβ. All reactions were performed at 30 °C for 10 min. Reactions were stopped by adding 5µL of phosphoric acid 0.8%. Aliquots (10 µL) were then transferred into a P30 Filtermat (PerkinElmer), washed five times with 0.5 % phosphoric acid and four times with water for 5 min. The filter was dried and transferred to a sealable plastic bag, and scintillation cocktail (4 mL) was added. Spotted reactions were read in a scintillation counter (Trilux, Perkinelmer). IC_{50} values were obtained according to Equation (1), where v is the measured reaction velocity, V is the apparent maximal velocity in the absence of inhibitor, I is the inhibitor concentration, and IC_{50} is the 50% inhibitory concentration.

$$v = V/\{1+(I/IC_{50})\} \quad (1)$$

Lipidic substrate preparation:

PI: phosphatidylinositol (Sigma); PS: 2-Oleoyl-1-palmitoyl-sn-glycero-3-phospho-L-serine (Sigma). PI and PS were dissolved in chloroform/methanol 9:1 and mixed at a 1:3 ratio. After chloroform/methanol evaporation, water was added to 1:62.5 w/v and the mixture sonicated to clarity.

Antiviral assays – materials and methods Assay preparation

Enterovirus (EV):

Rhabdosarcoma (RD) cells, Vero cells and Hela-Rh cells, subcultured in cell growth medium [MEM Rega3 (Cat. N°19993013; Invitrogen) supplemented with 10% FCS (Integro), 5 ml 200 mM L-glutamine (25030024) and 5 mL 7.5% sodium bicarbonate (25080060)] at a ratio of 1:4 and grown for 7 days in 150 cm^2 tissue culture flasks (Techno Plastic Products), were harvested and seeded in a 96-well plate at a cell density of 20 000 cells/well in assay medium (MEM Rega3, 2% FCS, 5 ml L-glutamine and 5 ml sodium bicarbonate) to perform standardized antiviral assay against EV71 and EVD68, CV and PV, RV02 and RV14, respectively.

Antiviral activity and cytotoxicity determinations

Compounds were prepared as DMSO stock solution with a final compound concentration of 10mM. The compound profiling setup was performed employing a Freedom EVO200 liquid handling platform (Tecan). The evaluation of the cytostatic/cytotoxic as well as the antiviral effect of each compound was performed in parallel within one run. Three 8-step 1-to-5 dilution series were prepared (starting from 100 µM) in assay medium added to empty wells (picornaviruses: 96-well microtiter plates, Falcon, BD) or in the medium present on top of pre-seeded cells. Subsequently, 50 µL of a 4x virus dilution in assay medium (assay medium supplemented with 15 ml $MgCl_2$ 1M (Sigma, M1028) in case of RV) was added followed by 50 µL of cell suspension. The assay plates were returned to the incubator for 2-3 (picornavirus, 35°C for RV) days, a time at which maximal cytopathic effect (CPE) for picornaviruses is observed.

For the evaluation of cytostatic/cytotoxic effects and for the evaluation of the antiviral effect in case of PV, CV, RV, the assay medium was replaced with 75 µL of a 5% MTS (Promega) solution in phenol red-free medium and incubated for 1.5 hours (37°C, 5% CO_2, 95-99%

relative humidity). Absorbance was measured at a wavelength of 498 nm (Safire2, Tecan) and optical densities (OD values) were converted to percentage of untreated controls.

Analysis of the raw data, quality control of each individual dose-response curve and calculation, if possible, of the EC_{50}, EC_{90} and CC_{50} values was performed employing ViroDM, a custom-made data processing software package. The EC_{50} and EC_{90} (values derived from the dose-response curve) represent the concentrations at which respectively 50% and 90% inhibition of viral replication would be observed. The CC_{50} (value derived from the dose-response curve) represents the concentration at which the metabolic activity of the cells would be reduced to 50 % of the metabolic activity of untreated cells.

The EC_{50}, EC_{90} and CC_{50} ± SD were, whenever possible, calculated respectively as the median of all the EC_{50}, EC_{90} or CC_{50} values derived from the 3 individual dose-response curves. The selectivity index (SI), indicative of the therapeutic window of the compound, was calculated as CC_{50}/EC_{50}. No further statistical analysis was performed.

CFTR assays

The effects of compounds on CFTR biogenesis and function were measured using assays exploiting CFTR fusion probes with anion-sensitive YFP[61] and pH-sensitive pHTomato.[62] Lipofectamine transfection was used for transient transfection of HEK293 cells. Cells plated in 96-well plates were incubated with the YFP-CFTR- or CFTR-pHTomato-encoding plasmid[48] using Lipofectamine 2000 (Life Technologies), according to manufacturer's instructions. Following transfection, cell plates were returned to the 37°C incubator for 24 h. Plates were further incubated at 30°C for 24 h prior to imaging, with or without additional drug treatment.

All imaging was carried out using ImageXpress (ImageXpress Micro XLS, Molecular Devices): an image-acquisition system equipped with a wide-field inverted fluorescence

microscope and fluidics robotics. Images were obtained with a 20X objective, using excitation/emission filters 472 ± 30 nm and 520 ± 35 nm, for YFP-CFTR and 531 ± 20 nm and 592 ± 20 nm for CFTR-pHTomato. In the latter assay, eGFP and Hoechst nuclear stain images were also acquired for each well, using excitation/emission filters 472 ± 30 nm and 520 ± 35 nm, and 377 ± 25 nm and 447 ± 30 nm, respectively. For each plate, the laser intensity and exposure were optimized to achieve the highest possible fluorescence whilst avoiding both photobleaching and saturation (illumination intensity 100-150/225 cd, and exposure 0.1 – 0.2 s)

For the YFP-CFTR assays, before imaging, cells were washed twice with 100 µl standard buffer (140 mM NaCl, 4.7 mM KCl, 1.2 mM $MgCl_2$, 5 mM HEPES, 2.5 mM $CaCl_2$, 1 mM Glucose, pH 7.4). Images were taken for 150 s at a frequency of 0.5 Hz. 50 µL extracellular I^- (as standard buffer with 140 mM NaCl replaced with 300 mM NaI; resulting in 100 mM final [I^-]) was added at 20 s, and activating compounds (50 µM Forskolin alone or together with 10 µM compounds for acute treatment) were added at 60 s. Maximum rate of iodide influx was used to quantify CFTR ion channel activity.[37]

For the CFTR-pHTomato assay, before imaging, cells were washed twice with 100 µL standard buffer (as above). During imaging, extracellular pH was changed using addition of 50 µL pH 6 buffer (as standard buffer, with 5 mM HEPES replaced with 10 mM MES: final [MES] 3.3 mM, ~ pH 6.5), and 50 µL pH 9 buffer (as standard buffer, with 5 mM HEPES replaced with 100 mM Tris: final [Tris] 25 mM, ~ pH 8.8). Two pHTomato images (acquisition frequency 0.5 Hz) were taken in each condition. To account for variation in transfection efficiency the pHTomato fluorescence was normalized using average fluorescence intensity of a soluble eGFP, co-expressed in the cytosol. Because the rise in pHTomato fluorescence falls largely within the 6.5 to 8.8 pH range,[63] the change in fluorescence obtained upon increasing extracellular pH ($\Delta F_{membrane}$) was used as an estimate of membrane-exposed CFTR.[37]

***In vivo* acute toxicity assay**

Animals

Male C57BL/6 mice (10–12 weeks old) (Charles River Laboratories, Calco, Italy), weighing 25-30g, were housed, five per cage, and maintained under standard conditions at our animal facility (12:12 h light–dark cycle, 22-24°C, food and water available ad libitum). Euthanasia was performed by CO_2 inhalation. All appropriate measures were taken to minimize pain or discomfort of animals. Animal experiments were performed according to the guidelines for the use and care of laboratory animals and they were authorized by the local Animal Care Committee "Organismo Preposto al Benessere degli Animali" and by Italian Ministry of Health "Ministero della Salute" (DL 26/2014).

Toxicity assay

After 4 hours fasting, **23a**, dissolved in carboxymethylcellulose and DSMO (90/10 for 20 and 60mg/kg; 66/34 at 180mg/kg) was subcutaneously (s.c.) administered at 20 (1 mouse/dose), 60 (1 mouse/dose) and 180mg/kg (3 mice/dose). Single mice were dosed in sequence at 48h intervals. A battery of tests to evaluate physical appearance and changes in unprovoked and provoked behaviour, motor activity, coordination and sensory/motor reflexes were carried out immediately before fasting, 1h and 24h after **23a** administration. Body weight was also assessed before and after fasting, prior to **23a** treatment or vehicle (n=5) (day 1), and daily thereafter for a total of 15 days.

Histology

Samples of lungs, liver and small intestine were harvested from vehicle-treated mice (n=2) and from mice administered with **23a** 180mg/kg s.c., 4h (n=3) and 72h (n=3) after compound

dosing. After euthanasia, mice were exsanguinated by cutting the caudal vena cava, the trachea was cannulated with PE-50 tubing and the lungs were fixed in situ via the cannula with 0.6 ml of 10% neutral buffered formalin, before the thorax was opened. Intestinal and liver tissues were excised and immediately immersion-fixed in 10% neutral buffered formalin overnight. For histological processing, the organs were dehydrated in graded ethanol series, clarified in xylene and paraffin embedded. 5 μm-thick sections were obtained through a rotary microtome (Slee Cut 6062, Slee Medical, Mainz, Germany). For the morphological evaluation, the sections were stained with haematoxylin and eosin, observed using a motorized microscope (Nikon Eclipse 90i, Nikon, Tokyo, Japan) equipped with a digital camera (Nikon model5M) and connected to a PC with image analysis software (NIS – Elements AR 3.1, Nikon Tokyo, Japan). The histological analysis was performed in blind by two independent researchers.

Supporting Information. The Supporting Information is available free of charge on the ACS Publications website at DOI: Synthesis and characterization of chemical intermediates; Molecular Formula Strings.

AUTHOR INFORMATION

Corresponding Author

*Prof. Marco Radi, Dipartimento di Scienze degli Alimenti e del Farmaco, Università degli Studi di Parma, Viale delle Scienze, 27/A, 43124 Parma, Italy. E-mail: marco.radi@unipr.it; phone: +39 0521 906080; fax: +39 0521 905006

Author Contributions

The manuscript was written by MR through contributions of all authors. All authors have given approval to the final version of the manuscript.

ACKNOWLEDGMENT

Work in MR laboratory and ST fellowship were supported by the University of Parma and Chiesi Foundation (Bando Dottorati di Ricerca 2014). EL was supported by grant 15UCL04, funded by the Sparks charity and Cystic Fibrosis Trust. EC was supported by AIRC grant MFAG (Id: 18811).

ABBREVIATIONS

CF, cystic fibrosis; CFTR, cystic fibrosis transmembrane conductance regulator; FEV, Forced Expiratory Volume; CPE, cytopathic effect; CVB3, coxsackievirus B3; EV, enterovirus; F508del, deletion of Phe 508; RV, human rhinovirus; PI, phosphatidylinositol; PI4K, phosphatidylinositol 4-kinase; PIP_2, phosphatidylinositol 4,5-bisphosphate; PIP_3, phosphatidylinositol 3,4,5-trisphosphate; PI4P, phosphatidylinositol 4-phosphate; TGN, trans-Golgi network.

REFERENCES

(1) Csanády, L.; Vergani, P.; Gadsby, D. C. Structure, gating, and regulation of the CFTR anion channel. *Physiol. Rev.* **2019**; *99*, 707-738.

(2) Denning, G. M.; Ostedgaard, L. S.; Welsh, M. J. Abnormal localization of cystic fibrosis transmembrane conductance regulator in primary cultures of cystic fibrosis airway epithelia. *J. Cell. Biol.* **1992**, *118*, 551-559.

(3) Du, K.; Sharma, M.; Lukacs, G. L. The DeltaF508 cystic fibrosis mutation impairs domain-domain interactions and arrests post-translational folding of CFTR. *Nat. Struct. Mol. Biol.* **2005**, *12*, 17-25.

(4) Sharma, M.; Benharouga, M.; Hu, W.; Lukacs, G. L. Conformational and temperature-sensitive stability defects of the delta F508 cystic fibrosis transmembrane conductance regulator in post-endoplasmic reticulum compartments. *J. Biol. Chem.* **2001**, *276*, 8942-8950.

(5) Deschamp, A. R.; Hatch, J. E.; Slaven, J. E.; Gebregziabher, N.; Storch, G.; Hall, G. L.; Stick, S.; Ranganathan, S.; Ferkol, T. W.; Davis, S. D. Early respiratory viral infections in infants with cystic fibrosis. *J. Cyst. Fibros.* **2019**, *in press*, doi: 10.1016/j.jcf.2019.02.004.

(6) Rossi, G. A.; Morelli, P.; Galietta, L. J.; Colin, A. A. Airway microenvironment alterations and pathogen growth in cystic fibrosis. *Pediatr. Pulmonol.* **2019**, *54*, 497-506.

(7) Kiedrowski, M. R.; Bomberger, J. M. Viral-Bacterial Co-infections in the Cystic Fibrosis Respiratory Tract. *Front. Immunol.* **2018**, 9:3067.

(8) Phan, H. Treatment complexity in cystic fibrosis (CF): An increasing multifaceted challenge. *Pediatr. Pulmonol.* **2018**, *53*, 1174-1176.

(9) Sawicki, G. S.; Goss, C. H. Tackling the increasing complexity of CF care. *Pediatr. Pulmonol.* **2015**, *50*, S74-S799.

(10) Sawicki, G. S.; Ren, C. L.; Konstan, M. W.; Millar, S. J.; Pasta, D. J.; Quittner, A. L. Treatment complexity in cystic fibrosis: trends over time and associations with site-specific outcomes. *J. Cyst. Fibros.* **2013**, *12*, 461-467.

(11) Kalaitzis, I. S.; Rowbotham, N. J.; Smith, S. J.; Smyth, A. R. Do current clinical trials in cystic fibrosis match the priorities of patients and clinicans? A systematic review. *J. Cyst. Fibros.* **2019**, in press, doi: 10.1016/j.jcf.2019.06.005.

(12) Van Goor, F.; Hadida, S.; Grootenhuis, P. D.; Burton, B.; Stack, J. H.; Straley, K. S.; Decker, C. J.; Miller, M.; McCartney, J.; Olson, E. R.; Wine, J. J.; Frizzell, R. A.; Ashlock, M.; Negulescu, P. A. Correction of the F508del-CFTR protein processing defect in vitro by the investigational drug VX-809. *Proc. Natl. Acad. Sci. U S A.* **2011**, *108*, 18843-18848.

(13) Sala, M. A.; Jain, M. Tezacaftor for the treatment of cystic fibrosis. *Expert. Rev. Respir. Med.* **2018**, *12*, 725-732.

(14) Ramsey, B. W.; Davies, J.; McElvaney, N. G.; Tullis, E.; Bell, S. C.; Dřevínek, P.; Griese, M.; McKone, E. F.; Wainwright, C. E.; Konstan, M. W., Moss, R.; Ratjen, F.; Sermet-Gaudelus, I.; Rowe, S. M.; Dong, Q.; Rodriguez, S.; Yen, K.; Ordoñez, C.; Elborn, J. S. et al. A CFTR potentiator in patients with cystic fibrosis and the G551D mutation. *N. Engl. J. Med.* **2011**, *365*, 1663-1672.

(15) Wainwright, C. E.; Elborn, J. S.; Ramsey, B. W.; Marigowda, G.; Huang, X.; Cipolli, M.; Colombo, C.; Davies, J. C.; De Boeck, K.; Flume, P. A.; Konstan, M. W.; McColley, S. A.; McCoy, K.; McKone, E. F.; Munck, A.; Ratjen, F.; Rowe, S. M.; Waltz, D.; Boyle, M. P. et al. Lumacaftor-Ivacaftor in Patients with Cystic Fibrosis Homozygous for Phe508del CFTR. *N. Engl. J. Med.* **2015**, *373*, 220-231.

(16) Jordan, C. L.; Noah, T. L.; Henry, M. M. Therapeutic challenges posed by critical drug-drug interactions in cystic fibrosis. *Pediat. Pulmonol.* **2016**, *51*, S61–S70.

(17) Cholon, D. M.; Quinney, N. L.; Fulcher, M. L.; Esther, C. R. Jr.; Das, J.; Dokholyan, N. V.; Randell, S. H.; Boucher, R. C.; Gentzsch, M. Potentiator ivacaftor abrogates pharmacological correction of deltaF508 CFTR in cystic fibrosis. *Sci. Transl. Med.* **2014**, *6*(246): 246ra296.

(18) Veit, G.; Avramescu, R. G.; Perdomo, D.; Phuan, P. W.; Bagdany, M.; Apaja, P. M.; Borot, F.; Szollosi, D.; Wu, Y. S.; Finkbeiner, W. E.; Hegedus, T.; Verkman, A. S.;

Lukacs, G. L. Some gating potentiators, including VX-770, diminish ΔF508-CFTR functional expression. *Sci. Transl. Med.* **2014**, *6*(246):246ra97.

(19) Carlile, G.W.; Yang, Q.; Matthes, E.; Liao, J.; Radinovic, S.; Miyamoto, C.; Robert, R.; Hanrahan, J. W.; Thomas, D. Y. A novel triple combination of pharmacological chaperones improves F508del-CFTR correction. *Sci. Rep.* **2018**, *8*(1),11404.

(20) Almand, E. A.; Moore, M. D.; Jaykus, L.-A. Virus-Bacteria Interactions: An Emerging Topic in Human Infection. *Viruses*, **2017**, *9*,(3), E58.

(21) Van Ewijk, B. E.; Wolfs, T. F. W.; Aerts, P. C.; Van Kessel, K. P. M.; Fleer, A.; Kimpen, J. L. L.; Van Der Ent, C. K. RSV Mediates Pseudomonas aeruginosa Binding to Cystic Fibrosis and Normal Epithelial Cells. *Pediatr. Res.* **2017**, *61*, 398-403.

(22) Tassini, S.; Sun, L.; Lanko, K.; Crespan, E.; Langron, E.; Falchi, F.; Kissova, M.; Armijos-Rivera, J. I.; Delang, L.; Mirabelli, C.; Neyts, J.; Pieroni, M.; Cavalli, A.; Costantino, G.; Maga, G.; Vergani,P.; Leyssen, P.; Radi, M. Discovery of Multi-Target Agents Active as Broad-Spectrum Antivirals and Correctors of Cystic Fibrosis Transmembrane Conductance Regulator (CFTR) for Associated Pulmonary Diseases. *J. Med. Chem.* **2017**, *60*, 1400−1416.

(23) Zambrowicz, B. P.; Sands, A. T. Modeling drug action in the mouse with knockouts and RNA interference. *Drug Discov. Today Targets* **2004**, *3*, 198–207.

(24) Deutschbauer, A. M.; Jaramillo, D. F.; Proctor, M.; Kumm, J.; Hillenmeyer, M. E.; Davis, R. W.; Nislow, C.; Giaever, G. Mechanisms of haploinsufficiency revealed by genome-wide profiling in yeast. *Genetics* **2005**, *169*, 1915–1925.

(25) H. Kitano, *Nat. Rev. Drug Discov.* **2007**, 6, 202-210.

(26) Csermely, P.; Agoston, V.; Pongor, S. *Trends Pharm. Sci.* **2005**, 26, 178-182.

(27) Pedemonte, N.; Lukacs, G. L.; Du, K.; Caci, E.; Zegarra-Moran, O.; Galietta, L. J.; Verkman, A. S. Small-molecule Correctors of Defective DeltaF508-CFTR Cellular

Processing Identified by High-Throughput Screening. *J. Clin. Invest.* **2005**, *115*, 2564−2571.

(28) Olivença, D. V.; Uliyakina, I.; Fonseca, L. L.; Amaral, M. D.; Voit, E. O.; Pinto, F. R. A Mathematical Model of the Phosphoinositide Pathway. *Sci. Rep.* **2018**, *8*:3099.

(29) Reuberson, J.; Horsley, H.; Franklin, R. J.; Ford, D.; Neuss, J.; Brookings, D.; Huang, Q.; Vanderhoydonck, B.; Gao, L. J.; Jang, M. Y.; Herdewijn, P.; Ghawalkar, A.; Fallah-Arani, F.; Khan, A. R.; Henshall, J.; Jairaj, M.; Malcolm, S.; Ward, E.; Shuttleworth, L.; Lin, Y.; Li, S.; Louat, T.; Waer, M.; Herman, J.; Payne, A.; Ceska, T.; Doyle, C.; Pitt, W.; Calmiano, M.; Augustin, M.; Steinbacher, S.; Lammens, A.; Allen, R. Discovery of a Potent, Orally Bioavailable PI4KIIIβ Inhibitor (UCB9608) Able To Significantly Prolong Allogeneic Organ Engraftment in Vivo. *J. Med. Chem.* **2018**, *61*, 6705-6723.

(30) Pranke, I.; Golec, A.; Hinzpeter, A.; Edelman, A.; Sermet-Gaudelus, I. Emerging Therapeutic Approaches for Cystic Fibrosis. From Gene Editing to Personalized Medicine. *Front. Pharmacol.* **2019**, *10*:121.

(31) Yoo, C. L.; Yu, G. J.; Yang, B.; Robins, L. I.; Verkmanb, A. S.; Kurth, M. J. 4'-Methyl-4,5'-bithiazole-based correctors of defective ΔF508-CFTR cellular processing. *Bioorg. Med. Chem. Lett.* **2008**, *18*, 2610–2614.

(32) Sander, T.; Freyss, J.; von Korff, M.; Rufener, C. DataWarrior: an open-source program for chemistry aware data visualization and analysis. *J. Chem. Inf. Model.* **2015**, *55*, 460-473.

(33) Tarcsay, Á.; Nyíri, K.; Keserű, G. Impact of lipophilic efficiency on compound quality. *J. Med. Chem.* **2012**, *55*, 1252-1260.

(34) Wymann, M. P.; Bulgarelli-Leva, G.; Zvelebil, M. J.; Pirola, L.; Vanhaesebroeck, B.; Waterfield, M. D.; Panayotou, G. Wortmannin Inactivates Phosphoinositide 3-Kinase by

Covalent Modification of Lys-802, a Residue Involved in the Phosphate Transfer Reaction. *Mol. Cell. Biol.* **1996**, *16*, 1722–1733.

(35) Pirrung, M. C.; Han, H.; Ludwig, R. T. Inhibitors of Thermus Thermophilus Isopropylmalate Dehydrogenase. *J. Org. Chem.* **1994**, *59*, 2430–2436.

(36) Li, X.; Zuo, Y.; Tang, G.; Wang, Y.; Zhou, Y.; Wang, X.; Guo, T.; Xia, M.; Ding, M.; Pan, Z. Discovery of a Series of 2,5-Diaminopyrimidine Covalent Irreversible Inhibitors of Bruton's Tyrosine Kinase with in Vivo Antitumor Activity. *J. Med. Chem.* **2014**, *57*, 5112–5128.

(37) Langron, E. Simone M. I.; Delalande, C. M.; Reymond, J. L.; Selwood, D. L.; Vergani, P. Improved fluorescence assays to measure the defects associated with F508del-CFTR allow identification of new active compounds. *Br. J. Pharmacol.* **2017**, *174*, 525-539.

(38) Okiyoneda, T.; Veit, G.; Dekkers, J. F.; Bagdany, M.; Soya, N.; Xu, H.; Roldan, A.; Verkman, A. S.; Kurth, M.; Simon, A.; Hegedus, T; Beekman, J. M.; Lukacs, G. L. Mechanism-based corrector combination restores deltaF508-CFTR folding and function. *Nat. Chem. Biol.* **2013**, *9*, 444-454.

(39) Loo, T. W.; Bartlett, M. C.; Clarke, D. M. Bithiazole correctors rescue CFTR mutants by two different mechanisms. *Biochemistry* **2013**, *52*, 5161-5163.

(40) Hanrahan, J. W.; Matthes, E.; Carlile, G.; Thomas, D. Y. Corrector combination therapies for F508del-CFTR. *Curr. Opin. Pharmacol.* **2017**, *34*, 105–111.

(41) Davison, H. R.; Taylor, S.; Drake, C.; Phuan, P. W.; Derichs, N.; Yao, C.; Jones, E. F.; Sutcliffe, J.; Verkman, A. S.; Kurth, M. J. Functional fluorescently labeled bithiazole ΔF508-CFTR corrector imaged in whole body slices in mice. *Bioconjug. Chem.* **2011**, *22*, 2593-2599.

(42) Baell, J. B.; Holloway, G. A. New substructure filters for removal of pan assay interference compounds (PAINS) from screening libraries and for their exclusion in bioassays. *J. Med. Chem.* **2010**, *53*, 2719−2740.

Table of Contents Graphic